Late-Holocene land surface change in a coupled social-ecological system, southern Iceland: a cross-scale tephrochronology approach

Author names:

Richard Streeter
Department of Geography and Sustainable Development, School of Geography and Geology, Irvine Building, St Andrews, KY16 9AL
rts3@st-andrews.ac.uk
Tel: 01334 463853

Andrew Dugmore
Institute of Geography, School of GeoSciences, Drummond Street, Edinburgh, EH8 9XP
Andrew.dugmore@ed.ac.uk
Tel: 0131 6508156

Corresponding author: Richard Streeter

Keywords: Grímsvötn, Iceland, soil erosion, Little Ice Age, resilience

Abstract
The chronological challenge of cross-scale analysis within coupled socio-ecological systems can be met with tephrochronology based on numerous well-dated tephra layers. We illustrate this with an enhanced chronology from Skaftártunga, south Iceland that is based on 200 stratigraphic profiles and 2635 individual tephra deposits from 23 different eruptions within the last 1140 years. We present new sediment-accumulation rate based dating of tephra layers from Grímsvötn in AD 1432±5 and AD 1457±5. These and other tephras underpin an analysis of land surface stability across multiple scales. The aggregate regional sediment accumulation records suggest a relatively slow rate of land surface change which can be explained by climate and land use change over the period of human occupation of the island (after AD ~870), but the spatial patterning of change shows that it is more complex, with landscape scale hysteresis and path dependency making the relationship between climate and land surface instability contingent. An alternative steady state of much higher rates of sediment accumulation is seen in areas below 300 m asl after AD ~870 despite large variations in climate, with two phases of increased erosion, one related to vegetation change (AD 870-1206) and another related to climate (AD 1597-1918). In areas above 300 m asl there is a short lived increase in erosion and related deposition after settlement (AD ~870-935) and then relatively little additional change to present. Spatial correlation between rates of sediment accumulation at different profiles decreases rapidly after AD ~935 from ~ 4 km to less than 250 m as the landscape becomes more heterogeneous. These new insights are only possible using high-resolution tephrochronology applied spatially across a landscape, an approach that can be applied to the large areas of the Earth's surface affected by the repeated fallout of cm-scale tephra layers.

1. Introduction

The long-term perspectives of Quaternary science offer much to the contemporary debates about landscape resilience and the drivers of land surface change (Dearing et al., 2010). Recent decades have seen significant progress in both the production of diverse proxy records of environmental change and the development of high-resolution, long-term time series (Bonnefille and Chalie, 2000; Brauer et al., 1999; Dansgaard et al., 1993; Marlon et al., 2008; Wang et al., 2001). High quality archives can now provide data with the sub-decadal, annual or seasonal resolution needed for the analysis of land surface changes on human timescales and assessments of possible interactions between environmental change and human societies (e.g., Dearing, 2008). However, while many fundamental challenges of temporal resolution have been tackled (Lowe et al., 2008; Ramsey, 2008), key issues of spatial resolution remain unsolved.

Land surface change can be driven at multiple scales. These can be both 'top-down' (as in the case of global scale processes that drive climate changes with local impacts) and 'bottom-up' (as in the case of small scale land use changes that in aggregate have regional effects). Precise and accurate chronologies applicable across a nested sequence of scales are necessary in order to make effective connections between global hypotheses, regional narratives and the detail of individual sites. The spatial and chronological challenges presented by the cross-scale analysis of land surfaces can be met with high-resolution tephrochronology which can define spatial patterns across scales from millimetres to hundreds of kilometres (Dugmore et al., 2009; Lowe, 2011; Streeter et al., 2012).

This approach can also be used to test how resilient the land surface has been to anthropogenic disturbance and climatic influences over millennial timescales. Resilient systems can tolerate a wide range of conditions and are likely to remain in a similar state through time (Scheffer et al., 2009). In contrast systems with low resilience are sensitive to changes in conditions and are likely to change state over time (c.f. Bhagwat et al., 2012). Changing resilience may explain why some perturbations produce large changes when earlier perturbations of similar magnitude produced little change (Scheffer et al., 2009). As resilience is scale dependent, effective resilience thinking requires engagement at the scale of enquiry, a scale above and a scale below (Walker et al., 2004). Enhanced resilience at one scale within a landscape may be directly related to reduced resilience at another scale. Within coupled social-ecological systems (SES) the relevant scales of enquiry are likely to be related to the scales of human use of the landscape (e.g., field systems, land holdings, community management of resources, regional networks of exchange).

In this paper we develop tephrochronology for the cross-scale analysis of land surface change. Tephra layers provide a limited number of discrete dates within a time series of data because of the episodic nature of volcanic eruptions, but tephrochronology provides unparalleled scope for precise and accurate 3-D reconstructions of change related to the isochrons formed by

tephra layers. This approach offers a hitherto largely untapped potential to develop understanding of the coupled interactions of environments and people, particularly those expressed as changing patterns of land surface change.

We focus on methodological issues of precision, accuracy, data density and statistical analysis related to the development of regional tephrochronology for multi-scale studies of land surface change over millennial timescales. We maximise the resolution of tephrochronology in Iceland by identifying patchy and marginal tephra layers and using high-resolution measures of sediment accumulation to provide calendrical dates. We use the example of landscape degradation to assess change at different spatial and temporal scales within a coupled SES and to address questions of long-term resilience of a land surface to changes in climate and vegetation cover.

2. Regional Setting

In order to develop new perspectives we focus on southern Iceland, one of the best locations in the world for applications of tephrochronology (Fig. 1), where changes in SESs and climate are expressed in land surface changes. Iceland is important for understanding the human impact on the environment because it was settled in comparatively recent historical times and so can provide accessible pre-human baselines. In addition the existence of the Landnám tephra (deposited 871± AD, Grönvold et al., 1995), which dates from immediately prior to Norse settlement, marks a precisely defined change from a purely ecological system to a combined social-ecological system.

The area east of Myrdalsjökull includes the areas of Skaftártunga, Mýrdalssandur, Eldhraun and Alfvanfrettur and extends from the southern coastal sandur of Iceland to the interior highlands (Fig. 1A). The sandur plains to the south of the study area have been frequently swept by jökulhlaups generated by the sub-glacial volcano Katla and covered by recent lava flows (most recently from eruptions of Eldgjá in AD ~935 (Larsen, 2000; Larsen, 2010) and Laki in AD 1783 (Thordarson and Self, 2003)). As a result they have a poorly developed vegetation cover. The neighbouring lowlands (< ~300 m asl) where present day farms are located are likely to have been dominated by *Betula* woodland before the Norse settlement of the late 9th century AD (Hallsdóttir, 1996; Lawson et al., 2007). Today, although areas of woodland survive, the landscape is dominated by forb meadowlands which have experienced differing degrees of sediment accumulation and soil erosion. The climate is cool, wet and windy. Mean annual temperatures at Kirkjubæjarklaustur weather station, 25 km east of the study area are 4.8°C (AD 1931-2009), precipitation is ~1700 mm/yr and mean annual wind speeds are 3.6 m/s.

Agriculture is based on a mix of introduced sheep, cattle, goats, horses, and in the early centuries of settlement, pigs (Dugmore et al., 2000; McGovern et al., 2007) Provisioning has always involved networks greater than that of the individual farms (Fig. 2).

We know settlement of Iceland was rapid (Vésteinsson and McGovern, 2012) and areas around farm sites experienced large ecological changes rapidly after Landnám (Hallsdóttir, 1996; Vickers et al., 2011). Evidence from the wider landscape shows that the change from a purely ecological system to a SES took place over several centuries, as shown by the centuries scale decline in woodland cover (Lawson et al., 2007; Church et al., 2007). This switch between dominant ecological processes to combined social-ecological processes was time transgresive.

Andisols are extensive in the region and highly susceptible to erosion because of their low cohesion (Arnalds et al., 2001). Iceland has experienced high levels of soil erosion since its settlement in AD ~870 (Dugmore et al., 2000; 2009; Streeter et al., 2012) and presently ~ 40% of rangeland grazing areas are classified as severely eroded (Arnalds et al., 2001). After the human colonisation of the island and the related introduction of terrestrial grazing mammals and subsequent anthropogenic reductions in woodland cover, soil erosion would have been driven by different processes, occurred in different patterns and had a different relationship to vegetation change than before Landnám. This is because people have created forb meadowlands, with different vulnerabilities to erosion, from areas of the landscape that would have naturally supported woodland. Generally the intensity of soil erosion (as measured by sediment accumulation rates) increased in the Little Ice Age (LIA) period (AD 1300–1900), although in part this is probably due to increased sediment supply due to erosion in lowland areas with deeper soils rather than increasing rates of areal denudation (Dugmore et al., 2009). Erosion typically proceeds by loss of area and a flip between alternate land surface states of stable vegetation cover and persistent soil erosion. Under deteriorating climate conditions or increased grazing pressure vegetation cover can develop erosion spots. These may coalesce to form labyrinths of exposed soils that in turn may widen to create metre-scale areas that are vulnerable to erosion by wind, frost and running water (Arnalds, 2000). Exposed sediment surfaces have a distinctive set of feedback loops and mutual dependencies so, once they develop, they may persist under much lower grazing intensities and milder climates than were needed to trigger their development in the first place. Denuding andisol surfaces have been an enduring feature of the Icelandic landscape since settlement and have been named *rofabards* (Arnalds, 2000). Therefore the breaching of vegetation cover can be considered a threshold between alternative land surface states (Dugmore et al., 2009).

Volcanic activity is very frequent in Iceland and often produces some form of tephra deposit (Haflidason et al., 2000). There is geological evidence or written accounts (or both) for over 200 eruptions since Landnám (Thordarson and Larsen, 2007). The exact number will never be known; but since two-thirds of the records come from the more recent half of the settlement period (post AD ~1500), when sources of evidence are more clear and abundant, the total is probably closer to 300 events. Most of the extensive tephra marker horizons found in post-Landnám sequences in Iceland have been dated with both precision and accuracy, most notably the tephras produced from Hekla and Katla (Thórarinsson, 1944; 1967; 1975).

The area east of Mýrdalsjökull has one of the most complete tephra records in Iceland and the tephra record in Alftaversafrettur (Fig. 1) extends back 8.4 ka (Larsen, 1984; Larsen, 2010; Larsen et al., 1999; Oladottir et al., 2005; Oladottir et al., 2008). Skaftártunga's proximity to the volcanic system of Katla (19-34 km) means that Katla is the source of the majority of tephras found here, but there are also tephras from Hekla (55-70 km), Veiðivötn (35-60 km), Eldjgá, (10-35 km), Öræfajökull (95-105 km) and Grímsvötn (87-105 km) (Thórarinsson 1958; Larsen, 1984, 2000; Larsen et al., 2001; Óladóttir et al., 2005, 2008). The stratigraphy and major element composition of the Katla tephras has been explored in detail (Óladóttir et al., 2005; 2008). The Grímsvötn volcanic system is the most active in Iceland, with 65 eruptions in historical times (from AD ~870 onwards) and seven in the period AD 1400-1480 (Larsen et al., 1998). The majority of tephras from these eruptions have only been found within the ice cap and have not produced widespread isopachs suitable for chronological control (Larsen et al., 1998; Steinthórsson, 1977). Within the post-Landnám tephra sequence, however there are two extensive layers originating from Grímsvötn and while these two tephras have been recorded previously in individual profiles (e.g. Larsen, 1981; Larsen, 2000; Oladottir et al., 2011b; Oladottir et al., 2005) their true extent is unclear. The eruption dates are not recorded in written records, but their stratigraphic position indicates they erupted between AD 1416–1477.

3. Methods

3.1 Recording of stratigraphic sections

Stratigraphic sections were recorded through soils and tephra sequences in Skaftártunga (Fig. 1d) between 57 m asl and 462 m asl, with mean altitude of 218 m. They were located on active eroding fronts and recent cuttings into surface sediments (e.g. ditches, road cuttings and actively eroding stream edges). Sections were cleared to a minimum width of 0.5 m. This was important because the thickness and the presence or absence of tephra layers varies over cm-scales due to both depositional effects at the time of the eruption, such as differences in vegetation cover, and due to post-depositional reworking for instance by cryoturbation processes (Dugmore and Newton, 2012; Kirkbride and Dugmore, 2005). Profiles were logged from the surface to the Landnám tephra layer (mean depth 1.1 m) to a resolution of ±2.5 mm, and ±1 mm for 27 sections recorded photogrammetrically. Tephra thickness within these sections was measured from scaled photographs allowing dozens to hundreds of measurements per layer (Streeter and Dugmore, 2013a). This is important because the considerable cm-scale variability commonly found in tephra layers makes collecting a representative measurement difficult without replication of measurements from an exposure of > 0.5 m width. For each tephra and sediment unit particle size and shape, layer colour and thickness, bedding, sediment sorting and the nature of stratigraphic contacts were noted. Where thickness varied substantially in sections not recorded photogrammetrically a representative thickness was determined by averaging three evenly spaced measurements across the section face, and the range of thickness recorded.

3.2 Field identification and sampling

One approach to recording tephra stratigraphy is to search for reference sections within sediment traps which might be expected to have a particularly complete record of tephra fall. Iceland is, however, a very dynamic landscape and tephra re-deposition can occur for a variety of reasons (Boygle, 1999; Dugmore and Newton, 2012) Thus we favour the creation of composite records based on many individual profiles. Key ‘marker horizons’ — easily field identifiable tephras that cover the entire study area — were identified from the published chronologies (Larsen, 2000; Óladóttir et al., 2005, see Table 1). We use the commonly applied Icelandic tephra layer naming convention of a letter indicating the volcanic system followed by year of eruption (e.g. K1416 the eruption of Katla in AD 1416) hereafter. Tephras were identified on the basis of their grain size and morphology, layer thickness and colour and stratigraphic location. All previously established tephra layer sources and ages were identified in the field and these identifications were confirmed with geochemical analysis in conjunction with their stratigraphic location (Streeter, 2011). Deposits that were not key markers were identified using mixture of field mapping and further selected geochemical analysis. Primary tephra layers were distinguished from andisols, other sediment and reworked material on the basis of lithology, grain morphology, spatial distribution and layer stratigraphy (Dugmore and Newton, 2012).

Using the stratigraphic framework of field identifiable tephras and the markers V1477 and K1416 it was possible to identify two tephra layers which occur frequently between AD 1416-1477. These had previously been recorded in individual sections as layers originating from Grímsvötn (e.g. Larsen, 1981; Larsen, 2000; Oladottir et al., 2005) but their spatial distribution has not been established. Samples of these tephra were collected from nine sections in Skaftártunga (Fig. 1C, SI. Table 1) and their distribution within recorded sequences mapped (Fig. 3, SI. Fig.1, SI. Fig. 2). In addition, closely related tephra layers of known age and origin (e.g. K1416, V1477 and K1500) were also collected in selected sections (see SI. Table 1).

3.3 Chemical analysis

Major and minor element analysis has been used to confirm the origins of selected tephras. Individual grains of glass from the tephras were analysed on a WDS Cameca SX100 electron microprobe, using the analytical protocols from Dugmore et al. (1995a). The analysing beam used an accelerating voltage of 15 keV, a beam diameter of 10 μm and a current of 2 nA for Na, Mg, Al, K, Ca, Fe and Si and 80 nA for P, Ti, Mn and P. The instrument was calibrated regularly against known standards (Supplementary Information) Optical examination in thin section was used to select 6-10 shards per sample for analysis that were not weathered and lacked crystalline inclusions. Only raw electron microprobe analysis with totals >97 wt% were utilised (Hunt and Hill, 1993). New data were compared with geochemical compositions for tephra from Icelandic volcanic systems (Tephrabase, www.tephrabase.org and published analysis Jakobsson, 1979; Larsen et al., 1999; 2001; Óladóttir et al., 2008; 2011a).

3.4 A 15th century sediment accumulation rate age model

At any one site the sediment accumulation rate (SeAR) is affected by regional sediment fluxes but the signal is dominated by the local geomorphic context (Dugmore and Erskine, 1994). Thus while many sections preserve a time dependant signal it is one that is highly spatially variable and this introduces a degree of noise. As we were interested in a time dependant processes (the accumulation of sediment) we focused on two sites where the preservation of tephra layers was especially good (Fig. 1c, profiles 153 and 179) and where the high SeARs (mean 0.55 mm/yr) ensured the vertical separation of layers that are closely spaced chronologically. As sediment accumulation in Iceland can vary greatly in the historical period (Dugmore et al., 2009; Dugmore and Buckland, 1991; Streeter et al., 2012) we selected sections where SeAR showed stability between K1262 and H1597 (Fig. 4a).

Our aim was to decrease the uncertainty in age estimations caused by cm-scale variability in tephra and sediment accumulation at any one particular site. We did this by using photogrammetric techniques, allowing hundreds of tephra thickness measurements to be taken from open sections by measuring thickness from scaled high-quality photographs (described in Streeter and Dugmore, 2013a). These techniques were used to collect measures of andisol accumulation between K1416 and the lower Grímsvötn tephra and between the upper Grímsvötn tephra and V1477 from two open sections (Fig. 1c, profiles 153 and 179). Linear accumulation rates were assumed between

K1416 and V1477, and this data was used to calculate an age estimate for each tephra based on its distance from a tephra of known age. Multiple measurements of sediment thickness (n=1960) from the 1 m wide sections give confidence in the mean age estimate and account for the effect of cm-scale variations in tephra thickness.

We checked that the selected sections were representative by comparing the calculated dates against SeAR from sections which were recorded using standard logging techniques (± 2.5 mm), where all four tephras were found, and where there was no indication of fluvial reworking (n=75). This gave a date within the error estimates of the calculated dates from the photogrammetrically recorded sections. The accuracy of this technique was further evaluated by dating a tephra of known age. The K1262 tephra was dated by inter calculating its age from the tephras H1206 and H1300 (time interval between control points 96 yr) using measurements to ±2.5 mm. The SeAR age calculated was AD 1264 ±10 (mean ±1SD, n=97).

3.5 Measuring landscape stability

Rates of aeolian sediment accumulation can be used as an indicator of geomorphic processes in the landscape (e.g. Thórarinsson, 1961a; Dugmore and Buckland, 1991; Gisladóttir et al., 2010). As the SeAR is a measure of aggradation at a site it reflects a wide range of Earth surface processes, not just land degradation or climate deterioration. These include the rate of sediment generation (by glacial, volcanic and fluvial processes), sediment transport rates and directions and the capability of a surface to trap sediment. It is likely that the relative influence of Earth surface processes will change between sites and through time. In particular the vegetation changes associated with the introduction of grazing livestock at Landnám, and the exploitation of woodlands probably changed the dominant sediment source in areas of human habitation (Dugmore et al., 2009).

Here sediment accumulation rate (SeAR) was calculated by measuring total sediment thickness between identifiable tephra layers. Based on a visual classification of particle size, accumulation was classified as aeolian material (fine sand–silts, <0.1 mm) or fluvial material (very coarse sands, >2 mm). Using this distinction local sediment fluxes (coarse material originating <250 m from profile) could be distinguished from regional aeolian signals (fine material, (Dugmore and Erskine, 1994). Large spatial variability between records of SeAR from closely spaced profiles indicates localised sources of sediment which the wind could move short distances, whereas similar records of SeAR from closely spaced profiles indicates a sediment source outwith the immediate area (Dugmore et al., 2009). This was evaluated here by plotting variograms indicating the dissimilarity of adjacent measurements of SeAR with increasing distance lags spaced at 250 m intervals. A spherical model was fitted to the empirical data, and the range (the distance lag at which correlation between sections is equal to correlation between global sections) calculated. The range indicates the distance at which SeAR in adjacent profiles is no longer correlated. Decreases in range represent periods where the level of spatial autocorrelation is reducing and the SeAR record becomes more spatially heterogeneous. This implies the drivers of SeAR are acting at

small scales (such as individual breaks in surface vegetation cover). If the range is increasing spatial autocorrelation is increasing and the drivers of SeAR may be acting at larger scales (such as climate).

In order to examine the changing relationships between SeAR and putative drivers of erosion they are plotted in phase space (c.f. Dearing, 2008). This approach can be used to provide evidence of alternative stable states (Wang et al., 2012). SeAR rates are calculated over periods bounded by dated tephas (e.g. SeAR is assumed to be constant between the tephras K1755 and H1845) so records which were based on annual or different time periods were averaged between the relevant dated tephras. The overall correlation between SeAR and temperature, storminess and levels of woodland cover was calculated using Pearson's *r* correlation coefficient. The dataset was weighted according to the number of sections recorded for each time period. In addition quantile regression (using the R package "quantreg", http://www.r-project.org/) was used to estimate trends at the 10%, 25%, 50%, 75% and 90% percentiles of the data points in order to investigate changing relationships between the variables through time.

4. Results

4.1 Tephrochronology

In total 2635 tephra units were identified from 200 stratigraphic sections. The majority of these were recorded to the depth of the Landnám tephra (AD 871±2, Grönvold et al., 1995), with 12 stratigraphic sections recorded to the SILK-LN tephra, extending the record to ~2.3–2.5 ka BP (Larsen et al., 2001). The chronology is described in Table I and contains four additional identified tephra layers from published chronologies for east of Mýrdarsjökull (e.g. Larsen, 2000). Three are previously unmapped tephras from Grímsvötn, and one is the extension of the visible extent of H1104 in the stratigraphy. In total 23 tephra can be found in the post-Landnám sequence, with on average 13 present. This provides an average effective resolution of ~90 years, and a maximum effective resolution of 50 years. The resolution between Landnám and AD 1300 is ~70 yrs and post AD 1300 it is ~40 yrs.

Based on high-resolution measurements of sediment accumulation from two sections (compared against lower resolution measurements from 75 sections) the date of the earlier Grímsvötn layer is AD 1432 ± 5 yrs (mean ±1SD) and the date of the later Grímsvötn layer is AD 1457 ±5 yrs (mean ±1SD) (Fig. 4).

4.2 Geochemistry and identification

Geochemical analysis confirmed the sequence of primary air fall tephra in the 15th century over this area was K1416, Grímsvötn (AD 1432±5), Grímsvötn (AD 1457±5), Veiðivötn (AD 1477) and Katla (AD 1500). In total 196 shards from the five sampled tephra layers were analysed (Fig. 5, Supplementary Information). The majority of samples had uniform geochemistry and individual shards showed little sign of mechanical weathering, supporting the field-based assumptions that these tephras are primary air fall and not

reworked material. Analysis of known layers (K1416, V1477, K1500) matched published compositions, confirming their field identification (Fig. 3, 5).

Samples which were field identified as Grímsvötn tephra based on their stratigraphic location had a TiO_2 content in the range 2.6–2.9% wt, lower than TiO_2 content of Katla tephra (3.1–5.1% wt), the most frequently found tephra in this area. A FeO/TiO_2 ratio of less than six indicates the tephra is not from the Bárdarbunga system (Óladóttir et al., 2011a). Therefore we believe that these two tephra both originate from Grímsvötn, rather than other volcanic systems under Vatnajökull. Full geochemical results from all Grímsvötn samples are presented in the Supplementary Information and online at Tephrabase (www.tephrabase.org, Newton et al., 2007).

4.3 Distribution of 15th century Grímsvötn tephra

Within the Skaftártunga region (Fig. 1C) the G1432±5 tephra has a mean thickness of 8 mm and was found in 47% of profiles, covering an area of ~240 km^2. It thickens towards the south (max thickness 20 mm) suggesting an axis of fall out south of Skaftártunga (SI. Fig 1). The G1457±5 tephra has a relatively uniform thickness (20 mm ±3.6 mm) within Skaftártunga (Fig. 1C). It was found in 74% of profiles. It covers a minimum area of ~260 km^2 (SI. Fig. 2).

4.4 Twelfth century tephras

Hekla AD 1104 is not noted in published chronologies (e.g., Larsen, 2000; Larsen et al., 2001; Óladóttir et al., 2005) but has been observed in some sections in this area (Larsen, 1979). Here it is found in 56 profiles north of 63°45'0 N. Based on stratigraphic position the Hekla AD 1158 tephra is a possible alternative interpretation for this tephra, however the geochemistry from profiles 17 and 20 (Fig. 1C) identifies this layer as being from the Hekla 1104 eruption (Supplementary Information). This improves our understanding of the presence of H1104 at the edge of its distribution.

In addition a thin (<5 mm), dark basaltic-intermediate tephra was found in 12 profiles between H1104 and K1206. One sample was analysed (10 shards, SI Table II). SiO_2 was 48-50%, and the FeO/TiO_2 ratio was 4.6–5.2 which means the tephra is not from Bardárbunga (Óladóttir et al., 2011a). We believe this tephra is also from Grímsvötn. We dated this tephra to AD 1160±20 (mean ±1SD) based on inter calculated rates of sediment accumulation. A Grímsvötn tephra of similar age is observed by Larsen (1984) in this area and a Grímsvötn tephra occurring directly above the Hekla 1158 tephra and within the calculated age range is present in 3 sections north-east of Vatnajökull and in a core from Lake Mývatn (Óladóttir et al., 2011a; Sigurgeirsson et al., 2013).

4.5 Spatial and temporal patterns in SeAR

The Landnám tephra provides a useful reference point for the start of human settlement and the introduction of grazing mammals. Prior to the Landnám tephra SeAR is dependant on climate but also the supply of sediment provided by volcanic eruptions, such as Hekla-4 which created a sediment pulse in lake records (Larsen et al., 2012). In the 12 stratigraphic

sections recorded to SILK-UN (917–777 BC, Larsen et al., 2001) SeAR is low (0.28 ±0.04 mm/yr) and exhibits little variability in time or at different altitudes (Fig. 8e). Six sections were recorded to SILK-LN (1512–1367 BC, Larsen et al., 2001) where SeAR is marginally lower (0.24 ±0.04 mm/yr).

There is a doubling in SeAR in the first 64 years after the Landnám tephra in all areas of the landscape. This change is especially pronounced in areas above 300 m asl, where SeAR is 0.77±0.4 mm/yr compared to 0.56±0.4 mm/yr below 300 m asl (Fig. 6a). This difference is notable because in general soil accumulation is lower and less variable above 300 m asl. On average 456±155 mm sediment is accumulated after AD 871 above 300 m asl compared to 780±576 mm below 300 m asl. The period immediately after settlement (AD 871–935) is the only period in the ~2.5 ka record when SeARs are greater above 300 m asl than below 300 m asl. However patterns of spatial autocorrelation (Fig. 7) indicate that sediment flux is relatively homogenous in this period and SeARs is similar across adjacent sections within ~4 km.

The period from AD 935–1206 has generally high SeAR, as well as a greater incidence of fluvial reworking visible in sections (Fig. 6B, 8E). The landholdings of Hrífunes and Flaga (57-212 m asl) show particularly high levels of SeAR during this period (Fig. 8f). The record becomes more spatially heterogeneous with much lower correlation in SeARs between closely spaced sections (Fig. 7). The highest SeARs are found below 300 m asl, below the probable upper altitude range of pre-Landnám forest cover (Thórhallsdóttir, 1997).

During the period AD 1206-1597 rates of SeAR decline to 0.50±0.3 mm/yr across all areas, and there is no significant difference between high altitude or low altitude areas (Fig. 6c, d). Spatial autocorrelation increases in the period AD 1389–1416 which suggests that regional drivers of erosion (such as climate) were more important than localised drivers (Fig. 7). However this signal is short lived and by late 15th century spatial correlation returns below 250 m. The period AD 1477–1500 has higher SeAR than the average for this period (Fig. 8E), but SeAR returns to average by the next dated tephra in AD 1597.

SeAR increases from the end of the 16th century to present, along with increases in indicators of instability (coefficient of variance and slope wash present within sections). The highest levels of SeAR are post AD 1918 (Fig. 8e, f, g) The highest pre-1918 SeARs are 2.4 times pre-Landnám levels and occur in AD 1845–1918, although the next highest SeARs (AD 1660-1755) are very similar (Fig. 6). After AD 1625 32% of profiles have SeARs more than double the post-Landnám mean of 0.55 mm/yr. Variability between SeAR at different sites as indicated by coefficient of variance increases from ~40% for the period AD 1416-1597 to 70–90% for AD 1597 to present. This increase in variability between profiles is reflected in measures of spatial autocorrelation which show no correlation of SeAR at adjacent sections above 250 m separation (Fig. 7).

Individual profiles show diverging patterns in SeAR, from unchanging rates prior to AD 1918 (Fig. 8g, profile 38) to systematic increases from AD 1597 to present, with SeAR levels going from ~0.6 mm/yr to ~2.2 mm/yr by the 19th century (Fig. 8g, profiles 148 and 151).

5. Discussion

5.1.1 Optimising tephrochronologies

South Iceland is an outstanding location for the application of tephrochronology and as such it is 'untypical' of volcanic areas in general, so approaches developed under such circumstances could be argued to lack wider relevance. However this is not the case. In order to acquire the best dating resolution possible we have utilised patchy and poorly defined layers, deposits that elsewhere are likely to hold the key for developing dating control that has the necessary granularity for effective analysis of combined social-ecological systems. Thus, the approaches used to optimise the Skaftártunga chronology could be important in the wider application of tephrochronology.

Maximising the resolution of teprochronologies relies on the identification and dating of as many isochronous tephra layers as possible. One strategy is to seek out cryptotephras (fine-grained tephras hidden from view within the stratigraphy), which are most frequently used to extend the spatial distribution of tephrochronology (Dugmore, 1989; Dugmore et al., 1995a, 1996; Hall and Pilcher, 2002; Hall, 2003; Swindles et al., 2011). In addition to cryptotephras, areas affected by repeated fallout often contain small visible layers of tephra that are of uncertain provenance and may be ignored but offer significant chronological potential. Examples of this are the two 15th century Grímsvötn tephra layers described in this paper. Securely identifying a minor tephra layer across the landscape requires a greater number of sites than a major tephra because its distribution is likely to be patchy. This patchiness means that a significant proportion of sites within the landscape will not contain a particular marginal tephra, even sites which are only short (50-100 m) distances apart. Thus single profile interpretations are likely to be of lower resolution. In this study the G1432±5 layer is present over the whole area but was only found in 47% of the profiles. This is probably due to differences in the depositional environment, post-depositional processes and local scale atmospheric effects, and has been observed elsewhere in Iceland (Boygle, 1999) and in cryptotephra (Lawson et al., 2012). With selective geochemical analysis (Fig. 5) and plotting of the stratigraphy (Fig. 3) these layers can be identified across a large number of sites and added to the regional tephrochronology.

While each in-situ tephra layer formed from atmospheric fallout defines an isochron, the most effective applications of tephrochronology require calendrical or sidereal dates. The best chronologies can come from a careful use of written sources, which can pin an age down to a particular hour — such as just after 9 am on the 19th May 1341 AD (Thórarinsson, 1967), Tephra layers unrecorded in reliable written sources maybe dated using other approaches such as radiocarbon dating (e.g. Dugmore et al., 1995b; Larsen et al., 2001) preferably within a Bayesian framework (Church et al., 2007), the counting of annual layers in ice caps (Steinthórsson, 1977; Gronvöld et al., 1995; Zielinski et al., 1995; Larsen et al., 1998; Vinther et al., 2006) and rythmites in lakes (Halflidason et al., 1992). Incremental dating methods may provide dating that approaches the accuracy and precision of the written record. Constraints on radiocarbon dating include the rarity of suitable organic remains within the ubiquitous andisols of historical-age contexts in Iceland.

These limitations are exacerbated by the constraints on radiocarbon in the recent past created by the Seuss effect. Sediment age-depth models inter-calculated from tephras of known age provide a possible solution (Óladóttir et al., 2005; 2011b; Sigurgeirsson et al., 2013), although they may also have large uncertainties associated with them as a result of the generally low-resolution measurements of sediment accumulation. When sediment age-depth models are calculated using many high-resolution measurements (Streeter and Dugmore, 2013a), and where the separation between securely dated horizons is small, this technique can provide dates with uncertainty in the order of a decade.

5.1.2 15th Century tephras

A key goal in the optimisation of tephrochronology is to trace each tephra layer over the greatest spatial extend possible. The G1457±5 tephra extends to Ketilsstaðir, Mýrdalur (Fig. 1c) where a tephra layer between the K1416 and K1500 tephras was identified by major element analysis as originating from Grímsvötn (Erlendsson et al., 2009). A field identified basaltic-intermediate tephra was found between the K1416 tephra and the V1477 tephra in 7 stratigraphic sections within 2 km of Ketilsstaðir. The position of these tephras in the stratigraphy indicates this is most likely to be the G1457±5 layer, although relatively small changes in accumulation rates would change this interpretation. Therefore the visible extent of the G1457±5 tephra in stratigraphic sections extends 135 km southwest of Grímsvötn. These tephra are not however found in sections around Eyjafjallajökull (Dugmore et al., 2013b) suggesting that Ketilsstaðir is close to the western edge of their visible distribution in areas to the south of Mýrdalsjökull.

G1432±5 and G1457±5 can be correlated with Grímsvötn tephra in a section 50 km east of Skaftártunga at Núpsstadarskógar (Fig. 1b, Óladóttir et al., 2011b). These tephras are between the K1417 and V1477 tephras and are dated to AD ~1430 and AD ~1450 based on a SeAR model (Óladóttir et al., 2011b). These dates are within the age estimates proposed in this paper but are only based on a limited number of measurements from a single profile. The thickness of both the upper and lower Grímsvötn layers is 4 cm at this location. Additional stratigraphic sections from around Vatnjajökull include Grímsvötn tephras which may be contemporaneous these two layers (Óladóttir et al., 2011b). However, only the Núpsstadarskógar section to the south-west of Vatnjajökull contains both Grímsvötn layers. As these sections are located closer to Grímsvötn these Grímsvötn tephras to the north and east of Vatnajökull may either 1) represent separate, smaller eruptions which produced limited tephra or 2) a minor axis of fallout from the same eruptions as considered here. Therefore it seems most likely that the major axis of tephra fall for both the G1432±5 and G1457±5 eruptions was to the south-west.

This detail matters because it 1) increases the confidence with which we can apply tephra to constrain environmental records and 2) can be used to understand more about the the tephra deposition itself and therefore our understanding of volcanic processes and eruptions.

5.2 Land surface change over 3.5ka

Overall pre-Landnám SeAR is similar to comparable areas of andisols around Eyjafjallajökull (0.2-0.3 mm/yr, Dugmore et al., 2000). There are fewer reliably dated tephras for the period prior to Landnám but we do not see any substantive change or trend in SeAR in the 2300 yrs in our record before Landnám. We see no signal of increased erosion as a result of periods of abrupt climatic cooling at 2.9 and 1.4 ka (Geirsdóttir et al., 2013; Larsen et al., 2012). This is in contrast to Icelandic lake records which do show increased sedimentation and changes in C:N ratios as a result of cooling at 2.9, 1.4 and 0.7 ka, the start of the LIA (Geirsdóttir et al., 2009; Geirsdóttir et al., 2013; Larsen et al., 2012). These lake records are interpreted as showing that soil erosion is predominately driven by climatic cooling and that there was no increase in sedimentation rates as a result of settlement in ~870 AD until the onset of the LIA. Geirsdóttir et al., (2013) find that from the period of 1 to 0.7 ka there was little to no soil erosion, which they attribute to the warm climate. In contrast our data shows high SeAR from 1.1 to 0.8 ka, at levels well outside the range seen in the previous 2500 yrs. This difference is probably a reflection of the very different environmental contexts of the records. Our sites are mostly below 400 m (mean 218 m asl) and < 10 km from farms and thus could be expected to best reflect environmental changes as a result of human settlement and the introduction of domestic livestock. The data used in Geirsdóttir et al., (2009) and Geirsdóttir et al., (2013) comes from lakes with high altitude catchments. Hvítárvatn is a proglacial lake at 422 m asl and one-third of its watershed is part of Langjökull ice cap (Larsen et al., 2012). It is sited in the interior highlands far from habitation. Haukadalsvatn has most of its catchment above 500 m asl. While these lakes provide excellent records of the processes operating within their comparatively high altitude catchments they have limited relevance for settled lowland areas.

The impact of tephra fall from the Eldgjá eruption in AD 933±1 (Vinther et al., 2006) would have been considerable in this area (Larsen, 2000). The average air fall depth of 210 mm would have been deep enough to smother vegetation and evidence of reworking by surface flow is more common immediately above the Eldgjá tephra than any other tephra in the sequence. However there is no correlation between depth of the Eldgjá tephra and SeAR at individual sections over the period to the next frequently present tephra (H1206). As the greatest depth of tephra fall is to the north, where both evidence of reworking is lower and SeAR rates are lower the higher SeAR in areas below 300 m asl does not appear to be related to the effects of the Eldgjá eruption. This pattern of higher SeAR and high rates of instability below 300 m asl continues to AD 1206, although where H1104 was recorded SeAR declines prior to H1206.

5.3 Cross scale analysis of environmental records

As the effective understanding of the resilience of SES requires a cross-scale analysis (Walker et al., 2004) there is a need for environmental records specific to a range of scales. Being able to resolve environmental change at the farm scale is important because many key actions take place at this scale (Lagerås, 2007) and these can lead to emergent behaviours across the wider

landscape. Although farms sites are the focus of individual archaeological excavations (e.g. Lucas, 2009), networks of resource use that encompass greater scales are known to be important for our effective understanding of the past (Lucas, 2009; McGovern et al., 2007, Dugmore et al., 2013a). An additional consideration is that the spatial scale of environmental records may not match with the scales of social organisation of the landscape use (Fig. 2), and records are often located far from sites of human habitation. Unlike environmental archives wedded to particular natural catchments, the soil records considered here may be grouped in ways that reflect the social organisation of the landscape, such as areas landholdings with contrasting patterns of land management (Fig. 2, Fig. 8f).

Switching from the high temporal resolution but limited spatial resolutions of regional environmental archives to the varied spatial scale of SES (Fig. 2) adds uncertainty. North Atlantic SST records (Fig. 8a) and storminess records (Fig. 8b) have annual resolution but poor discrimination at sub-regional spatial scales. Lake records have high temporal resolution but spatially homogenise records at the scales encompassed by their catchments (Fig. 8c, d). Tephrochronology used in isolation cannot match the continuous temporal resolution of annually-laminated environmental archives (such as ice cores) but it can provide precise and accurate spatial correlations at a near continuous range of spatial resolutions. This can be used to reduce the uncertainty involved when assessing change across different spatial scales.

Our data reinforces the idea that particular drivers of land surface change may only operate in specific areas of the landscape. If datasets do not capture records from these specific areas they may give a misleading impression of what is driving environmental change. The mismatch will be greatest where conditions are heterogeneous and environmental signals are transmitted only short distances. This is the case for soil erosion in south Iceland, particularly after the 10th century where the spatial correspondence between sites is typically less than 250 m (Fig. 7). Multiple soil profiles will record localised erosion in different areas of the landscape at different times, and this is seen in systematic patterns of change such as erosion zones migrating down slope, or erosion that reflects patterns of deforestation. In contrast a lake record contains a homogenised signal generated by changes across the altitudinal range of the catchment and across all its ecological and land management zones. The lake records considered by Geirsdóttir et al., (2009), for example, reflect an amalgamated record of a catchment where the largest area is above 500 m asl (Fig. 8C). As much of this catchment lies above the natural tree line (~300 m asl in south Iceland (Thórhallsdóttir, 1997)) it is perhaps not surprising that the high levels of sediment flux in sites below 300 m asl over the period 1.1–0.7 ka in our data are not found in the Geirsdóttir et al (2009) record. Furthermore because the sediment pulse observed in our data in sites > 300 m asl is short lived (< 64 yrs) it may be smoothed out in records where there is not secure chronological controls bracketing this particular period.

5.4 Resilience, alternative stable states and land degradation

Multiple explanations for the observed pattern of SeAR in south Iceland have been identified previously, each applying to discrete areas or periods of time

(e.g. Dugmore and Buckland, 1991; Dugmore et al., 2009; Streeter et al., 2012; Streeter and Dugmore, 2013a). If these alternative (but complimentary) explanations are placed in the theoretical framework of complex systems, resilience, alternative stable states and thresholds then apparent inconsistences can be resolved. The SeAR record compared to other environmental records (Fig. 8) suggests changing spatial relationships between climate, geomorphic and human processes through time. These relationships can be assessed as phase diagrams (c.f. Dearing, 2008). Changes in SeAR through time can be shown against some of the main putative drivers of land surface change, temperature, storminess, and vegetation change (Fig. 9). The levels of SeAR suggest alternative stable states within certain parts of the land surface system because there are clusters of data and there is no regular progression.

Aggregate SeAR plotted against a low-frequency North Atlantic palaeo-climatic reconstruction (Mann et al., 2009) shows a strong phase organisation pattern because there are trajectories of change (Fig. 9a). Prior to Landnám SeAR is insensitive to climatic variability. The introduction of grazing animals at Landnám and the creation of persistent areas of aeolian erosion moves SeAR into a new regime of consistently higher SeARs, and there is little overlap between SeARs before and after Landnám (Streeter et al., 2012). This new phase state of elevated SeAR is reached after a rapid transition period (< 64 yrs), which is plausible considering that Iceland was colonised rapidly by a people dependent upon introduced domesticated animals (Vésteinsson and McGovern, 2012) and we know that woodland around farms was cleared rapidly (Halsdóttir, 1996; Vickers et al., 2011). The introduction of wide-ranging herbivorous mammals and the related systematic removal of woodland represents a fundamental shift in the ecology of the island. An alternate state of SeAR does not occur in areas above 300 m asl, which, apart from the first 60 years after settlement, shows a continuity of SeAR levels without obvious step-wise shifts. This contrast between low lying and upland areas may be due to a lack of pre-existing sediment cover for sustained erosion at these elevations (Dugmore et al., 2009).

After Landnám a generally cooling climate between AD 871–1477 is associated with reducing SeAR rates (Fig. 9). From AD 1625-1918 climate is variable, with significant cold periods and with an overall higher SeAR than the earlier period. This increase in sediment flux after AD 1625 is absent in sites > 300 m asl. The periods of highest SeARs do not correlate to those of the lowest temperature at sites below 300 m (Fig. 10). Although at low levels of SeAR (10% quantile) there is a weak negative correlation with temperature overall there is a weakly positive correlation, with a strong correlation at the 90% quantile ($r=0.81$, $n=37$, $p=0.29$), although these correlations are not significant (Fig. 10). This pattern is counterintuitive because lower temperatures result in shorter growing seasons and they could be reasonable associated with increased grazing pressures. These observations are not consistent with existing mainly climatic explanations of soil erosion in other areas of Iceland (Axford et al., 2009; Geirsdóttir et al., 2009) and is counter to our understanding of the physical surface process and constraints on vegetation growth which point to higher rates of erosion in cooler, windier

climates (e.g. Arnalds et al., 2012). One possible mechanism is that in lowland areas reducing winter snow cover exposes larger areas of sediment to needle ice formation, which significantly increases the susceptibility of andisols to wind erosion (Arnalds et al., 2012). Therefore one interpretation of these contrasting patterns is that it reflects changing sensitivities to temperature over time. Where SeARs (and thus areas of exposed sediment) are low soil erosion increases as temperature declines, and this matches with pre-Landnám records of erosion (Axford et al., 2009; Geirsdóttir et al., 2009). However when SeARs are high, reflecting extensive exposed sediments, this relationship with temperature becomes weaker or may even be reversed. It suggests that at the landscape scale, the relationship between climate, vegetation cover and SeAR is complex, contingent on past states and their legacies, and sensitive to other changes in the coupled SES, particularly changes in livestock management.

The Na+ record in the GISP2 ice core provides a proxy for storminess in the north Atlantic (Meeker and Maywski, 2002). The period of human habitation in Iceland can be split into an earlier, calmer period (until AD ~1425) and a later, stormier period (AD ~1425–1900) (Dugmore et al., 2007). This is not reflected in SeAR rates which do not meaningfully correlate with this storminess index at any altitude ($r = -0.05$, $n=36$, $p = 0.76$), indicating that there is no simple relationship between how often and how hard the wind blows and the volumes of sediment eroded.

Vegetation change as a result of land management is a likely driver of soil erosion because of the strong feedback loops and mutual dependencies between vegetation cover and Earth surface processes (Marston, 2010). In our datasets, changes in woodland cover inferred from the best current long term record of *Betula* pollen decline (Lawson et al., 2007) provide a strong organisation in phase space below 300 m asl. SeAR are high during the prolonged decline of woodland cover from settlement times until the 14th Century. Once an essentially ‘treeless’, open landscape is created after AD 1300 SeAR moves within a small range between 0.45–0.6 mm/y, with the exception of three time periods where it increases to around 0.7 mm/y. These excursions correspond to climatically cool periods. In general there is a weakly negative non-significant relationship between tree cover and SeAR (Fig. 10). Above 300 m, the approximate local limit of natural woodland in south Iceland (Thórhallsdóttir, 1997), regional changes in *Betula* abundance do not correlate with changes in SeAR. The lack of this pre-LIA, but post-settlement, period of high SeAR in other areas (e.g. Ólafsdóttir and Guòmundsson, 2002; Gísladottir et al., 2010, Brown et al., 2012) could be due to regional differences in pre-existing woodland cover. Where woodland cover was already low at the time of settlement resilience to grazing by domestic animals may have been greater, despite less favourable ecological conditions (Mairs et al., 2006).

The phase diagrams also provide evidence of multi-century landscape scale hysteresis. The settlement of Iceland created a fundamental change of SeAR from persistently low pre-existing rates to an alternative state where fluxes increased to almost double the pre-Landnám rate. In the late 16th century this

regime shifted again to a state of even higher rates – a change that is persisting despite temperatures that are likely to be warmer than those at the time of initial settlement. The most probable explanations for these changes are firstly the introduction of grazing animals and secondly the propagation of erosion fronts into deep lowland soils where they are maintained by positive feedback loops (Dugmore et al., 2009).

5.5 Implications for sustainability science

There is increasing recognition that long time perspectives, such as those considered here, are essential to understand current and future landscape resilience because past landscape trajectories affect future pathways of change (Dearing et al., 2010). There is also strong evidence that early warning signals exist in a range of environmental systems that may be identified in time-series of data (Scheffer et al., 2009; Scheffer et al., 2012; Wang et al., 2012; Streeter and Dugmore, 2013b). In addition to single point records, changes in spatial patterning have the potential to provide early warning signals and a measure of system resilience (Dai et al., 2013; Scheffer et al., 2012; Guttal and Jayaprakash, 2008; Kéfi et al., 2007). Increased variance (greater spatial heterogeneity) could be a signal of reduced resilience in the system, and an example of critical slowing down to perturbations (e.g. Dakos et al., 2011). This is also related to the connectivity of different components of the system. In southern Iceland, soil erosion commonly proceeds along erosion 'fronts' (rofabards) and greater variation may be associated with reduced resilience because it implies a larger area of exposed andisol available to be eroded by surface processes. Although increasing spatial correlation is also related to reduced resilience (Dai et al., 2013) and may be a better indicator than temporal series (Guttal and Jayaprakash, 2008), it is likely this variance would be found at a smaller scale than considered here. In principle, however, the spatial records of tephrochronology could be used to investigate spatial indicators of changing land surface resilience.

Erosion rates as reflected in SeAR do not change markedly in Skaftártunga during the period AD 1206–1597, despite social and economic upheaval (Karlsson, 2000) and known periods of cool and stormy climate comparable in magnitude to those that occur after AD 1597 and which are associated with high SeAR. It is probably, however, that soil cover experienced a gradual loss of area through the migration of erosion fronts. It is also likely that each of these periods of stress caused a spatially-specific and partial loss of resilience that collectively built to lead to an overall loss of resilience in the landscape system as a whole. This loss of resilience is exemplified by the much higher rates of SeAR experienced in current mild climatic conditions than earlier periods of similar climatic conditions, suggesting the present situation of elevated SeAR represents an alternative stable state and that soil erosion may have a different response to temperature change than earlier in the Holocene. Our research shows that climate change alone does not drive soil erosion and climate amelioration alone is unlikely to inhibit degradation. It is unwise therefore, to assume that a key driver of past erosion was climate deterioration and also unwise to assume that climate amelioration will present

an easy solution to degradation and a straight-forward (or indeed inevitable) route to landscape remediation.

6. Conclusion

The application of resilience thinking to records of environmental change requires spatially extensive chronologies that are precise and accurate. This can be achieved across scales of tens of metres to tens of kilometres with high-resolution regional tephrochronologies. This approach allows the assessment of landscape resilience at multiple scales and may be employed to tackle questions of human-environment interaction that would be difficult to address in any other way, highlighting the importance of tephrochronology in the large areas of the earth affected by repeated episodes of identifiable volcanic fallout.

Patchy proximal tephra deposits may be used to develop spatially extensive high-resolution chronologies. These types of high-resolution, spatial records are especially well suited to resilience analysis in coupled social ecological systems because they can be used at multiple scales within the landscapes where people live.

Tephra deposits can be dated to high-resolution using sediment accumulation rates where SeARs are high, measurements are precise and numerous and the stratigraphic separations between securely dated horizons are small (equivalent decadal time scales). Two tephras from Grímsvötn are dated to AD 1432±5 and AD 1457±5 and mapped over 240 km^2. The area where the G1457±5 tephra is visible in stratigraphic sections probably extends to Mýrdalur, 200 km south-west of Grímsvötn caldera.

Aggregate soil profile records suggest a relatively slow rate of land surface change which can be explained by climate and land use change over the post-Landnám period, but the spatial patterning and phase relationships show that it is more complex, with landscape scale hysteresis and path dependency making the relationship between climate and SeAR contingent.

Extensive soil erosion started immediately after the settlement of Iceland and continues today, with periods of particularly high erosion from AD 871–1206 and AD 1597-present. However, the rates and severity of erosion have varied spatially. In the first decades of settlement (AD ~870–935) erosion was most extensive in upland areas that lacked woodland cover (> 300 m asl). Ecological change from woodland to grassland driven by the grazing pressures of introduction livestock was probably responsible for a phase of lowland erosion from AD 935–1206. Erosion rates declined over the period AD 1206–1597 but then increased to reach their maximum pre-1918 levels in the late 17th century and in the second half of the 19th century. Climate cooling and increased storminess in the LIA is likely to have been the key driver for post AD 1597 land surface change by increasing the frequency and rate of erosion processes and increasing relative grazing pressures through reduced biomass production. These changes highlight the varying resilience of the landscape and hysteresis of erosion over millennial timescales.

Acknowledgements

This research was supported by a UK Natural Environment Research Council (NERC) PhD studentship (NE/F00799X/1) and a US National Science Foundation Arctic Research Council Grants OPP 0352596; OPP 02900001 and OPP 0732327. Tephra samples were analysed at Edinburgh University Tephra Analytical Facility supported by NERC, and we would like to thank Chris Hayward for assistance with the analysis and Anthony Newton for assistance with preparing the samples. We would also like to thank landowners in Skaftártunga who granted permission to dig sections, especially Bergdís Jóhannsdóttir and Sigurður O. Pétursson at Búland and Elín Þorgeirsdóttir at Hrífunes. Lastly, we thank the two anonymous reviewers for their helpful and detailed comments.

References

Adalsteinssion, S., 1990. Importance of sheep in early Icelandic agriculture. Acta Archaeologica 61, 285-291

Arnalds, O., 2000. The Icelandic 'rofabard' soil erosion features. Earth Surface Processes and Landforms 25(1), 17–28.

Arnalds, O., Thorarinsdottir, E., Metusalemsson, S., Jonsson, A., Gretarsson, E., Arnason, A. 2001. Soil erosion in Iceland. Tech. rept. (English translation of original Icelandic publication from 1997.) Soil Conservation Service and Agricultural Research Institute, Reykjavik, Iceland 121 pp.

Arnalds, O., Gisladottir, F.A., Orradottir B., 2012. Determination of aeolian transport rates of volcanic soils in Iceland. Geomorphology 167-168, 4-12.

Axford, Y., Geirsdóttir, Á., Miller, G.H., Langdon, P.G., 2009 Climate of the Little Ice Age and the past 2000 years in northeast Iceland inferred from chironomids and other lake sediment proxies. Journal of Paleolimnology 41, (1), 7-24.

Bhagwat, S.A., Nogué, S., Willis, K.J., 2012. Resilience of an ancient tropical forest landscape to 7500 years of environmental change. Biological Conservation 153, 108-117.

Bonnefille, R., Chalie, F., 2000. Pollen-inferred precipitation time-series from equatorial mountains, Africa, the last 40 kyr BP. Global and Planetary Change 26, 25-50.

Boygle, J., 1999. Variability of tephra in lake and catchment sediments, Svínavatn, Iceland. Global and Planetary Change 21, 129–149.

Brauer, A., Endres, C., Gunter, C., Litt, T., Stebich, M., Negendank, J.F.W., 1999. High resolution sediment and vegetation responses to Younger Dryas climate change in varved lake sediments from Meerfelder Maar, Germany. Quaternary Science Reviews 18, 321-329.

Brown, J.L., Simpson, I.A., Morrison, S.J.L., Adderley, W.P., Tisdall, E., Vésteinsson, O. 2012. Shieling Areas: Historical Grazing Pressures and Landscape Responses in Northern Iceland. Human Ecology 40, 81-99

Church, M., Dugmore, A., Mairs, K. A., Millard, A., Cook, G., Sveinbjarnardottir, G., Ascough, P., Roucoux, K.H., 2007. Charcoal Production during the Norse and Early Medieval periods in Eyjafjallahreppur, Southern Iceland. Radiocarbon 49 (2), 659–672.

Dai, L., Korolev, K.S., Gore, J. (2013) Slower recovery in space before collapse of connected populations. Nature 496, 355-358.

Dansgaard, W., Johnsen, S.J., Clausen, H.B., Dahljensen, D., Gundestrup, N.S., Hammer, C.U., Hvidberg, C.S., Steffensen, J.P., Sveinbjornsdottir, A.E., Jouzel, J., Bond, G., 1993. Evidence for general instability of past climate from a 250-KYR ice-core record. Nature 364, 218-220.

Dakos, V., Kéfi, S., Rietker, M., van Nes, E.H., Scheffer, M., 2011. Slowing Down in Spatially Patterned Ecosystems at the Brink of Collapse. American Naturalist 177(6),153-166.

Dearing, J.A., 2008. Landscape change and resilience theory: a palaeoenvironmental assessment from Yunnan, SW China. The Holocene 18, 117-127.

Dearing, J.A., Braimoh, A.K., Reenberg, A., Turner, B.L., van der Leeuw, S., 2010. Complex land systems: the need for long time perspectives to assess their future. Ecology and Society 15(4), 21.

Dugmore, A.J. 1989. Icelandic volcanic ash in Scotland. Scottish Geographical Magazine 105, 168–172.

Dugmore, A.J., Buckland, P., 1991. Tephrochronology and late Holocene soil erosion in Southern Iceland. In: Maizels, J.K., Caseldine, C., *(*eds.*)* Environmental Change in Iceland: Past and Present*,* Kluwer Academic*,* 147-159.

Dugmore, A.J., Erskine, C.C., 1994. Local and regional patterns of soil erosion in southern Iceland. Münchener Geographische Abhandlungen. 12, 63-79.

Dugmore, A.J., Larsen, G., Newton, A.J., 1995a. Seven Tephra Isochrones in Scotland. The Holocene 5(3), 257–266.

Dugmore, A., Cook, G., Shore, J., Newton, A., Edwards, K., Larsen, G., 1995b. Radiocarbon dating tephra layers in Britain and Iceland. Radiocarbon, 37(2), 379–388.

Dugmore, A.J., Newton, A.J., Edwards, K.J., Larsen, G., Blackford, J.J., Cook, G.T., 1996, Long-distance marker horizons from small-scale eruptions: British tephra deposits from the AD 1510 eruption of Hekla, Iceland. Journal of Quaternary Science, 11, 511–516.

Dugmore, A.J., Newton, A., Larsen, G., Cook, G., 2000. Tephrochronology, Environmental Change and the Norse Settlement of Iceland. Environmental Archaeology, 5, 21–34.

Dugmore, A.J., Borthwick, D.M., Church, M.J., Dawson, A., Edwards, K.J., Keller, C., Mayewski, P., McGovern, T.H., Mairs, K., Sveinbjarnardóttir, G. 2007. The Role of Climate in Settlement and Landscape Change in the North Atlantic Islands: An Assessment of Cumulative Deviations in High-Resolution Proxy Climate Records. Human Ecology 35(2), 169-178.

Dugmore, A.J., Gisladóttir, G., Simpson, I.A., Newton, A., 2009 Conceptual Models of 1200 Years of Icelandic Soil Erosion Reconstructed Using Tephrochronology. Journal of the North Atlantic 2(1), 1-18.

Dugmore, A.J., Newton, A., 2012. Isochrons and beyond: maximising the use of tephrochronology in geomorphology. Jökull 62, 39-52.

Dugmore, A.J., McGovern, T.H., Streeter, R.T., Madsen, C.K., Smiarowski, K., Keller, C. 2013a. 'Clumsy solutions' and 'Elegant failures': Lessons on climate change adaptation from the settlement of the North Atlantic islands. In: Sygna, L., O'Brian, K., Wolf, J. (Eds.), A Changing Environment for Human Security: A Transformative Approaches to Research, Policy and Action: Routledge, Oxford. 435-451

Dugmore, A.J., Newton, A.J., Smith, K.T., Mairs, K.-A., 2013b. Tephrochronology and the late Holocene volcanic and flood history of Eyjafjallajokull, Iceland. Journal of Quaternary Science 28, 237-247.

Erlendsson, E., Edwards, K,J., Buckland, P.C., 2009. Vegetational response to human colonisation of the coastal and volcanic environments of Ketilsstaðir, southern Iceland. Quaternary Research. 72, 174-187.

Geirsdóttir, A., Miller, G.H., Thordarson, T., Olafsdottir, K.B., 2009. A 2000 year record of climate variations reconstructed from Haukadalsvatn, West Iceland. Journal of Paleoolimnology 41, 95-115.

Geirsdóttir, Á., Miller, G.H., Larsen, D.J., Ólafsdóttir, S., 2013. Abrupt Holocene climate transitions in the northern North Atlantic region recorded by synchronized lacustrine records in Iceland. Quaternary Science Reviews 70, 48-62.

Gísladóttir, G., Erlendsson, E., Lal, R., Bigham, J., 2010. Erosional effects on terrestrial resources over the last millennium in Reykjanes, southwest Iceland. Quaternary Research 73, 20-32.

Guttal, V., Jayaprakash, C., 2008. Changing skewness: an early warning signal of regime shifts in ecosystems. Ecology Letters 11, 450-460.

Grönvold, K., Óskarsson, N., Johnsen, S.J., Clausen, H.B., Hammer, C.U., Bond, G., Bard, E., 1995. Ash layers from Iceland in the Greenland GRIP ice core correlated with ocean and land sediments. Earth and Planetary Science Letters 135, 149–155.

Hall, V.A., 2003. Vegetation history of mid- to western Ireland in the 2nd millennium AD; fresh evidence from tephra-dated palynological investigations. Vegetation History and Archaeobotany, 12(1), 7–17.

Hall, V.A. Pilcher, J.R., 2002. Late-Quaternary Icelandic tephras in Ireland and Great Britain: detection, characterization and usefulness. The Holocene 12, 223-230.

Hallsdóttir, M., 1996. Frjógreining. Frjókorn sem heimild um landnámid. In: Grímsdóttir, G.Á., (ed.). Um Landnám Á Íslandi. Societas scientiarum Islandica, Reykjavík, 123–34.

Haflidason, H., Larsen, G., Ólafsson, G., 1992. The recent sedimentation history of Thingvallavatn, Iceland. Oikos 64, 80–95.

Haflidason, H., Eiriksson, J. and Kreveld, S.V., 2000. The tephrochronology of Iceland and the North Atlantic region during the Middle and Late Quaternary: a review. Journal of Quaternary Science, 15(1), 3-22.

Hunt, J., Hill, P.G. 1993. Tephra geochemistry: a discussion of some persistent analytical problems. The Holocene, 3(3), 271–278.

Jakobsson, S.P., 1979. Petrology of Recent basalts of the Eastern Volcanic Zone, Iceland. Acta Naturalia Islandica, 26, 1–103.

Karlsson, G. 1996. Plague without rats + Examining the course and histories of severe epidemics and outbreaks of pneumonic plague in isolated medieval communities: The case of 15th-century Iceland, Journal of Medieval History 22, 263-284

Karlsson, G., 2000. Iceland's 1000 years: History of a Marginal Society. Hurst & Company, London.

Kéfi, S, Rietkerk, M., Alados, C.L., Pueyo, Y., Papanastasis, V.P., Elaich, A., de Ruiter, P.C., 2007. Spatial vegetation patterns and imminent desertification in Mediterranean arid ecosystems. Nature 449(7159), 213-217.

Kirkbride, M.P., Dugmore, A.J., 2005. Late Holocene solifluction history reconstructed using tephrochronology. In: Harms, C., Murton, J.B., *(*ed.*)* Cryospheric Systems: Glaciers and Permafrost, Geological Society*,* London, 145-155.

Larsen, D.J., Miller, G.H., Geirsdóttir, Á., Ólafsdóttir S., 2012. Non-linear Holocene climate evolution in the North Atlantic: a high-resolution, multi-proxy record of glacier activity and environmental change from Hvítárvatn, central Iceland. Quaternary Science Reviews 39, 14-25.

Larsen, G., 1979. Um aldur Eldgjárhrauna (Tephrochronological dating of the Eldgjá lavas in S-Iceland, in Icelandic). Náttúrufræðingurinn 49, 1–25.

Larsen, G., 1981. Tephrochronology by Microprobe Glass Analysis, In: Self, S., Sparks, R.S.J. (Eds.), Tephra Studies. Springer Netherlands, pp. 95-102.

Larsen, G., 1984 Recent volcanic history of the Veidivötn fissure swarm, Southern Iceland. An approach to volcanic risk assessment. Journal of Volcanology and Geothermal Research 22, 33-58.

Larsen, G., 2000. Holocene eruptions within the Katla volcanic system, south Iceland: Characteristics and environmental impact. Jökull, 49, 1–28.

Larsen, G., Gudmundsson, M.T., Bjornsson, H., 1998. Eight centuries of periodic volcanism at the center of the Iceland hotspot revealed by glacier tephrostratigraphy. Geology 26, 943–946.

Larsen, G., Dugmore, A., Newton, A., 1999. Geochemistry of historical-age silicic tephras of Iceland. The Holocene 9(4), 463–471.

Larsen, G., Newton, A., Dugmore, A., Vilmundardottir, E., 2001. Geochemistry, dispersal, volumes and chronology of Holocene silicic tephra layers from the Katla volcanic system, Iceland. Journal of Quaternary Science, 16(2), 119–132.

Larsen, G., 2010. 3 Katla: Tephrochronology and Eruption History, In: Anders Schomacker, J.K., Kurt, H.K. (Eds.), Developments in Quaternary Sciences. Elsevier, pp. 23-49.

Lagerås, P., 2007. The Ecology of Expansion and Abandonment: Medieval and Post-Medieval Land-use and Settlement Dynamics in a Landscape Perspective. Riksantikvarieämbetet.

Lawson, I.T., Gathorne-Hardy, F.J., Church, M.J., Newton, A.J., Edwards, K.J., Dugmore, A.J., Einarsson, A., 2007. Environmental impacts of the Norse settlement: palaeoenvironmental data from Mývatnssveit, northern Iceland. Boreas 36(1), 1–19.

Lawson, I.T., Swindles, G.T., Greenberg, D., Plunkett, G., 2012. The spatial distribution of Holocene cryptotephras in north-west Europe since 7 ka: Implications for understanding ash fall events from Icelandic eruptions. Quaternary Science Reviews 41, 57-66.

Lowe, D.J., 2011. Tephrochronology and its application: A review, Quaternary Geochronology 6(2), 107-153.

Lowe, J.J., Rasmussen, S.O., Bjorck, S., Hoek, W.Z., Steffensen, J.P., Walker, M.J.C., Yu, Z.C., Grp, I., 2008. Synchronisation of palaeoenvironmental events in the North Atlantic region during the Last Termination: a revised protocol recommended by the INTIMATE group. Quaternary Science Reviews 27, 6-17.

Lucas, G. (ed) 2009. Hofstadir: excavations of a Viking Age feasting hall in north-eastern Iceland. Fornleifastofnun Íslands (Institute of Archaeology, Iceland). Reykjavik.

Mairs, K. A., Church, M.J., Dugmore A.J., Sveinbjarnardottir, G., 2006. Degrees of success: evaluating the environmental impacts of long term settlement in south Iceland. In *The Dynamics of Northern Societies*, Arneborg J, Grønnow B (eds). PNM, Publications from the National Museum, Studies in Archaeology and History, 10: Copenhagen: 363–371.

Mann, M.E., Zhang, Z., Rutherford, S., Bradley, R.S., Hughes, M.K., Shindell, D., Ammann, C., Faluvegi, G., Ni, F., 2009. Global Signatures and Dynamical Origins of the Little Ice Age and Medieval Climate Anomaly. Science 326, 1256-1260.

Marlon, J.R., Bartlein, P.J., Carcaillet, C., Gavin, D.G., Harrison, S.P., Higuera, P.E., Joos, F., Power, M.J., Prentice, I.C., 2008. Climate and human influences on global biomass burning over the past two millennia. Nature Geoscience 1, 697-702.

Marston, R.A., 2010. Geomorphology and vegetation on hillslopes: Interactions, dependencies, and feedback loops. Geomorphology 116, 206-217.

Meeker, L.D., Mayewski, P.A., 2002. A 1400-year high-resolution record of atmospheric circulation over the North Atlantic and Asia. The Holocene 12, 257-266.

McGovern, T.H., Perdikaris, S., Einarsson, A. Sidell J., 2006. Coastal connections, local fishing, and sustainable egg harvesting: patterns of Viking Age inland wild resource use in Myvatn district, Northern Iceland. Environmental Archaeology, 11(2), 187-205.

McGovern, T.H., Vésteinsson, O. Fridriksson, A., Church, M.J., Lawson, I., Simpson, I.A., Einarsson, A., Dugmore, A.J., Cook, G.T., Perdikaris, S., Edwards, K.J., Thomson, A., Adderly, W.P., Newton, A.J., Lucas, G., Edvardsson, R., Aldred, O., Dunbar, E., 2007. Landscapes of Settlement in Northern Iceland: Historical Ecology of Human Impact and Climate Fluctuation on the Millennial Scale. American Anthropologist 109 (1), 27-51.

Moberg, A., Sonechkin, D.M., Holmgren, K., Datsenko, N.M., Karlén, W. 2005. Highly variable Northern Hemisphere temperatures reconstructed from low- and high-resolution proxy data. Nature, 433, 613-617.

Newton, A. J., Dugmore, A. J. and Gittings, B. M. 2007. Tephrabase: tephrochronology and the development of a centralised European database. Journal of Quaternary Science 22, 737–743

Óladóttir, B.A., Larsen, G., Thordarson, T., Sigmarsson, O., 2005. The Katla volcano S-Iceland: Holocene tephra stratigraphy and eruption frequency. Jökull 55, 53–74.

Óladóttir, B., Sigmarsson, O., Larsen, G., Thordarson, T., 2008. Katla volcano, Iceland: magma composition, dynamics and eruption frequency as recorded by Holocene tephra layers. Bulletin of Volcanology 70, 475–493.

Óladóttir, B, A., Sigmarsson, O., Larsen, G., Devidal, J.L., 2011a. Provenance of basaltic tephra from Vatnajökull subglacial volcanoes, Iceland, as determined by major- and trace-element analyses. The Holocene 21(7), 1037-1048.

Óladóttir, B., Larsen, G., Sigmarsson, O., 2011b. Holocene volcanic activity at Grímsvötn, Bárdarbunga and Kverkfjöll subglacial centres beneath Vatnajökull, Iceland. Bulletin of Volcanology 73(9), 1187-1208.

Ólafsdóttir, R., Guómundsson, H.J., 2002. Holocene land degradation and climatic change in northeastern Iceland. Holocene, 12(2), 159–167.

Ramsey, C.B., 2008. Deposition models for chronological records. Quaternary Science Reviews 27, 42-60.

Scheffer, M., Bascompte J., Brock, W.A., Brovkin, V., Carpenter, S.R., Dakos, V., Held, H., van Nes, E.H., Rietkerk, M., Sugihara, G., 2009. Early-warning signals for critical transitions. Nature 461, 53-59

Scheffer, M., Carpenter, S.R., Lenton, T.M., Bascompte, J., Brock, W., Dakos, V., van de Koppel, J., van de Leemput, I.A., Levin, S.A., van Nes, E.H., Pascual, M., Vandermeer, J., 2012. Anticipating Critical Transitions. Science 338(615), 344-348.

Sigurgeirsson, M.Á., Hauptfleisch, U., Newton, A., Einarsson, Á., 2013. Dating of the Viking Age Landnám Tephra in Lake Myvatn Sediment. Journal of the North Atlantic, 21, 1-11.

Steinthórsson, S., 1977. Tephra Layers in a Drill Core from the Vatnajökull Ice cap. Jökull, 27, 2–27.

Streeter, R.T., 2011. Tephrochronology, landscape and population: impacts of plague on medieval Iceland. Unpublished PhD thesis. The University of Edinburgh.

Streeter, R., Dugmore, A.J., Vésteinsson, O., 2012. Plague and landscape resilience in premodern Iceland. Proceedings of the National Academy of Sciences 109(10), 3664-3669.

Streeter, R., Dugmore, A.J., 2013a. Reconstructing late-Holocene environmental change in Iceland using high-resolution tephrochronology. The Holocene 23(2),197-207.

Streeter, R., and Dugmore, A.J., 2013b. Anticipating land surface change. Proceedings of the National Academy of Sciences. 110(15), 5779-5784.

Swindles, G.T., Lawson, I.T., Savov, I.P., Connor, C.B., Plunkett, G., 2011. A 7000-yr perspective on volcanic ash clouds affecting Northern Europe. Geology 39, 887-890.

Thordarson, T., Self, S., 2003. Atmospheric and environmental effects of the 1783–1784 Laki eruption: A review and reassessment. Journal of Geophysical Research: Atmospheres 108, 4011.

Thordarson, T., Larsen, G., 2007. Volcanism in Iceland in historical time: Volcano types, eruption styles and eruptive history. Journal of Geodynamics 43. 118-152.

Thórarinsson, S., 1944. Tefrokronoliska studier pa Island (Tephrochronological studies in Iceland). Geografiska Annaler, 26, 1–217.

Thórarinsson, S., 1958. The Öræfajökull eruption of 1362. Vol. II. Acta Naturalia islandica.

Thórarinsson S., 1961a. Uppblástur á Island í ljósi öskulagarannsókna (Wind erosion in Iceland. A tephrochronological study). Ársrit Skó græktarfëlags Islands, 17-54.

Thórarinsson S., 1961b. Population changes in Iceland. Geographical Review, 51(4), 519-533

Thórarinsson, S., 1967. The Eruptions of Hekla in historical times. The Eruption of Hekla 1947-1948. 1.

Thórarinsson. S., 1975. Katla og annáll Kötlugosa. Árbók Ferðafélags Íslands.

Thórhallsdóttir, T.E., 1997. Tundra Ecosystems of Iceland, In: Wielgolaski, F.E. (Ed.), Polar and Alpine Tundra. Elsevier, Amsterdam, pp. 85-96.

Vésteinsson, O., McGovern, T.H., 2012. The Peopling of Iceland, Norwegian Archaeological Review, 45:2, 206-218.

Vickers, K., Erlendsson, E., Church, M., Edwards, K.J., Bending, J. 2011. 1000 years of environmental change and human impact at Stóra-Mörk,

southern Iceland – a multiproxy study of a dynamic and vulnerable landscape The Holocene 21(6), 979-995.

Vinther, B. M., Clausen, H.B., Johnsen, S.J., Rasmussen, S.O., Anderson, K.K., Buchardt, S.L., Dahl-Jensen, D., Seierstad, I.K., Siggaard-Andereson, J.P., Steffensen, J.P., Svensson, A., Olsen, O., Heinemeier, J. 2006. A synchronized dating of three Greenland ice cores throughout the Holocene. Journal of Geophysical Research 111, 1-11.

Wang, R., Dearing, J.A., Langdon, P.G., Zhang, E., Yang, X., Dakos, V., Scheffer, M., 2012. Flickering gives early warning signals of a critical transition to a eutrophic lake state. Nature 492, 419-422.

Wang, Y.J., Cheng, H., Edwards, R.L., An, Z.S., Wu, J.Y., Shen, C.C., Dorale, J.A., 2001. A high-resolution absolute-dated Late Pleistocene monsoon record from Hulu Cave, China. Science 294, 2345-2348.

Walker, B., Holling, C.S., Carpenter, S.R., Kinzig, A., 2004. Resilience, adaptability and transformability in social–ecological systems. Ecology and Society 9(2), 5.

Zielinski, G.A., Germani, M.S., Larsen, G., Baillie, M.G., Whitlow, S., Twickler, M.S., Taylor, K., 1995. Evidence of the Eldgjá (Iceland) eruption in the GISP2 Greenland ice core: relationship to eruption processes and climatic conditions in the tenth century. The Holocene 5(2), 129-140.

Captions

Figure 1 - Study area. Overview location (a) with location of proxy records in Fig. 8 and 9. Location of Grímsvötn (b) and section with Grímsvötn layers described in this paper. Location of sampled tephras (c), stratigraphic section numbers correspond to those in SI. Table I. Profiles 153 and 179 were used to calculate ages for the two undated Grímsvötn tephras (Fig. 4). (d) Location of stratigraphic sections with major rivers and landholdings also shown. Farms in parenthesis are abandoned. Pre-settlement woodland is generally found at less than 300 m asl (Thórhallsdóttir, 1997): extent of woodland cover on sandur unknown prior to settlement.

Figure 2 –Spatial scales over which socio-ecological systems in Iceland operate. Fodder is produced in the home fields of the farm and was a key determinant of success because fodder was necessary to sustain livestock through the winter (Adalsteinsson, 1990). In the past natural wet meadows were harvested and outlying shielings or summer farms extended the utilisation of the upland resources. Rangeland grazing is managed at the multi-farm (*hreppur*) scale. Regional exchange networks have included birds, eggs, fish, marine mammals and essential fuel resources such as peat and charcoal (McGovern et al., 2006; 2007).

Figure 3. Sub-sections showing the period from AD 1389–1625 from sections which had samples taken for geochemical analysis. Sections are arranged from north to south (left-right) with the distance in km between profiles shown by the scale bar. Further sample details in SI. Table I. Profile numbers correspond to those in Fig. 1a. The source volcanic system based on geochemistry is indicated next to sampled layers.

Figure 4 – Box plots showing estimated age of the Grímsvötn tephras. (a) Shows the SeAR for profiles selected for photogrammetric measurements (Streeter and Dugmore, 2013a). (b) Shows calculated age of the tephras based on linear sediment accumulation rates between the Katla AD 1416 tephra and the Veiðvötn AD 1477 tephra. Bold vertical line shows median calculated age and the large solid circle the mean age. Small circles are outliers. Dates were calculated using photogrammetric measurements from profile 179 and 153. These dates were cross checked against lower resolution measurements (±2.5 mm) from 75 other profiles where all four tephra layers were present, but were not used as part of the final age calculation.

Figure 5. Major element plot of sampled 15th century tephra layers east of Mýrdalsjökull. For the location of the samples refer to SI. Table 1 and Fig. 1 and 3 and full results are in SI. Table II. Shaded reference areas are based on Jakobsson (1979) and Tephrabase (www.tephrabase.org).

Figure 6 – Sediment accumulation rates by altitude for five periods, based on known tephra markers (Table I). Bold red lines are smoothed loess filters (bandwidth 0.4) and open red circles indicate sections with indications of fluvial reworking. (a) Pre-Landnám SeAR and SeAR for the first 65 years after settlement, with relatively high rates in areas above 300 m, a similar pattern to elsewhere in south Iceland (Dugmore and Buckland, 1991). (b) In the first ~300 yrs of human settlement the highest levels SeAR are found below 300 m asl, with more periods of fluvial reworking than in earlier periods. Panels c, d and e show a flat altitudinal trend, with SeAR increasing only slightly in the LIA (e), with increased variability.

Figure 7 - Binned empirical variograms of spatial correlation in SeAR for 10 time periods based on widely occurring tephras (Table I). Bold lines are fitted spherical models, with grey shaded area indicating the range for the model. Initially erosion is spatially correlated for distances up to 4 km but by the 13th century there is no correlation above 250 m separation (the smallest correlation considered in the analysis). This continues through to the present, with the exception of the period AD 1389–1416, over which patterns of correlation increase to 1.5 km, which may be due to a general reduction in landscape pressure due to plague reducing population in AD 1402–1404 (Streeter et al., 2012, Streeter and Dugmore, 2013a). After this period spatial correlation is < 250 m to AD 1918 as the sediment flux becomes increasingly heterogeneous.

Figure 8 – Multiple proxies of environmental change in Iceland AD 700–2000. (a) Two multi-proxy temperature reconstructions, North Atlantic sea surface temperatures (SST, Mann et al., 2009) and Moburg et al., (2005). (b) Shows

GISP2 Na+ deviations from the mean, a proxy for storminess (Meeker and Mayeskwi, 2002). Cumulative deviations from the mean show a shift to stormier and windier conditions around AD 1425 (Dugmore et al., 2007). (c) Changes in total organic carbon at Lake Haukadalsvatn, west Iceland used as a proxy for aeolian erosion (Geirsdóttir et al., 2009). Bold horizontal bars show means over periods matching key tephra horizons in study (see Table I). (d) Woodland cover is represented by *Betula* pollen percentages from a lake core near Lake Mývatn, north Iceland (Lawson et al., 2007) and charcoal pits present in south Iceland (Church et al., 2007) (e) Mean aggregate SeAR from Skaftártunga for period separated by dated tephra layers, with 1 standard deviation show by grey shading. Mean calculated where n =>10. (f) Mean aggregate SeAR at the scale of the landholding, from two small landholdings (Hrífunes and Flaga, see Fig. 1d). (g) Change in SeAR at the landscape scale, 2 stratigraphic sections which record the onset of increased erosion at AD 1597, but profile 38 shows stability through the entire settlement period prior to AD 1918. (h) Population trends in Iceland. Prior to the first census in AD 1703 estimates are based on medieval populations being similar to or even higher than the population in AD 1703 (Thórarinsson, 1961b; Karlsson, 2000). Plague reductions of ~40% in AD 1402–1404 and ~30% in AD 1496 are shown (Karlsson, 1996).

Figure 9 – Phase diagrams showing factors affecting SeAR over the past 2000 years for all sites (a), below 300 m asl (b) and above 300 m asl (c). Proxy records for temperature, storminess and woodland cover were averaged over periods bounded by dated tephra layers (see Table I). Temperature record is North Atlantic SST from Mann et al., 2009. Storminess is Na+ proxy from GISP2 ice core (Meeker and Mayskwi, 2002). Woodland cover is *Betula Pubescens* from a lake core near Mývatn (Lawson et al., 2007).

Figure 10 – Quantile regression plots of the relationship between rates of sediment accumulation and putative drivers of soil erosion. (a) SeAR is plotted against North Atlantic SST from Mann et al., 2009. (b) SeAR is plotted against a measure of woodland cover (*Betula* pollen % from Lawson et al., 2007). (c) SeAR plotted against a measure of storminess, Na+ ppb from the GISP2 ice core (Meeker and Mayeskwi, 2002). Grey lines show 0.10, 0.25, 0.75 and 0.90 quantile regressions, black line is median regression and dashed line shows the least-squares estimated regression.

Supplementary Information Caption

SI. Figure 1. The thickness of 1432±5 Grímsvötn tephra's at each section location.

SI. Figure 2. The thickness of 1457±5 Grímsvötn tephra's at each section location.

Table I

Table 1 – Tephra layers used

Tephra	Date	Reference
Katla 1918*	1918 AD	Thórarinsson 1975
Hekla 1845	1845 AD	Thórarinsson 1967
Laki-Grímsvötn 1783	1783 AD	Thórarinsson 1967
Katla 1755*	1755 AD	Thórarinsson, 1975
Katla 1660	1660 AD	Thórarinsson, 1975
Katla 1625*	1625 AD	Thórarinsson, 1975
Katla 1612	1612 AD	Thórarinsson, 1975
Hekla 1597	1597 AD	Thórarinsson, 1967
Katla 1500	1500 AD	Larsen, 1984; Larsen, 2000
Veðivötn 1477	1477 AD	Larsen, 1984
Grímsvötn 1457±5	1457±5 AD	SeAR age this study, ~1460 AD Óladóttir et al, 2011b
Grímsvötn 1432±5	1432±5 AD	SeAR age this study, AD ~1430 Óladóttir et al, 2011b
Katla 1416*	1416 AD	Larsen, 2000
Hekla 1389	1389 AD	Thórarinsson, 1967
Öræfajökull 1362	1362 AD	Thorarinsson, 1958
Hekla 1341	1341 AD	Thórarinsson, 1967
Hekla 1300	1300 AD	Thórarinsson, 1967
Katla 1262*	1262 AD	Thórarinsson, 1975; Larsen, 2000
Hekla 1206*	1206 AD	Thórarinsson, 1967
Grímsvötn 12thC	~1140–1180	This paper#
Hekla 1104	1104 AD	Thórarinsson, 1967
Eldgjá (E935)*	934–938 AD, 933±1 in Greenland ice core	Larsen 2000; Vinther et al., 2006
Landnám*	871±2	Grönvold et al., 1995
SILK-UN	2660±50 BP	Larsen et al. 2001
SILK-LN	3139±40 BP	Larsen et al. 2001

* Key marker horizons used in the study

This may be from the same eruption which produces a Grímsvötn tephra to the north of Vatnajökull at this time, Óladóttir et al., 2011b.

Figure 1

Click here to download high resolution image

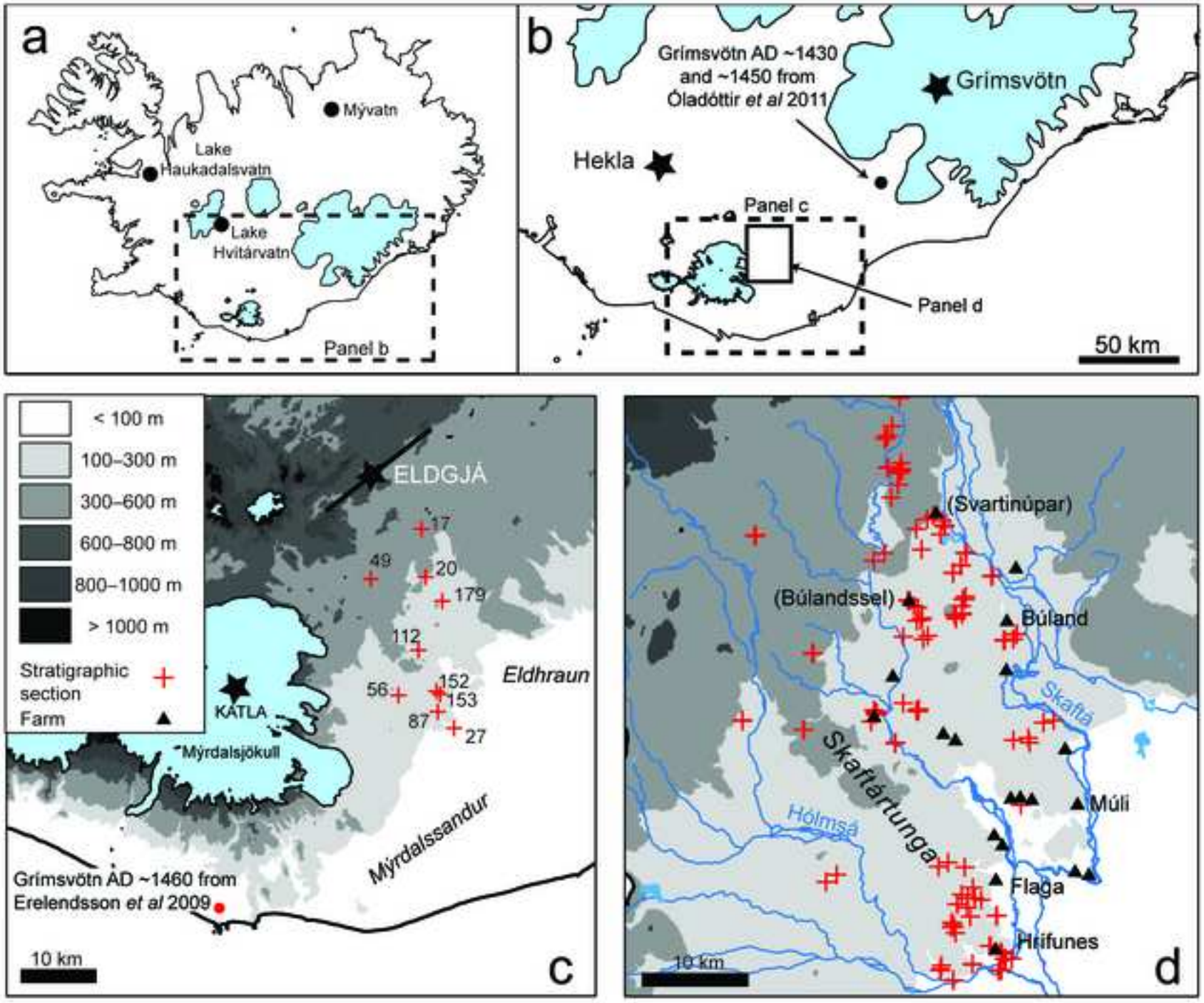

*Figure 2

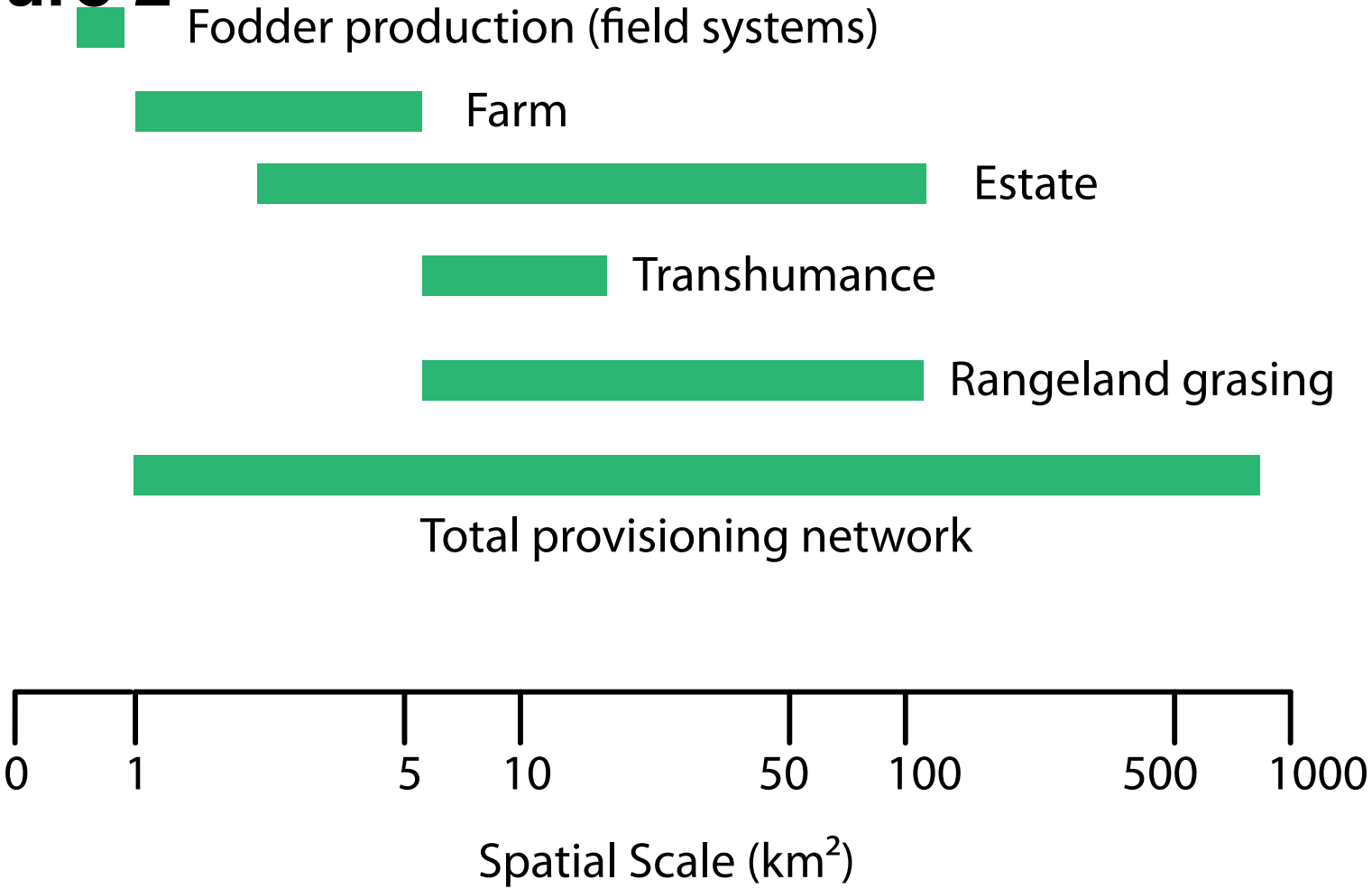
Fodder production (field systems)
Farm
Estate
Transhumance
Rangeland grasing
Total provisioning network
0
1
5
10
50
100
500
1000
Spatial Scale (km²)

Figure 3

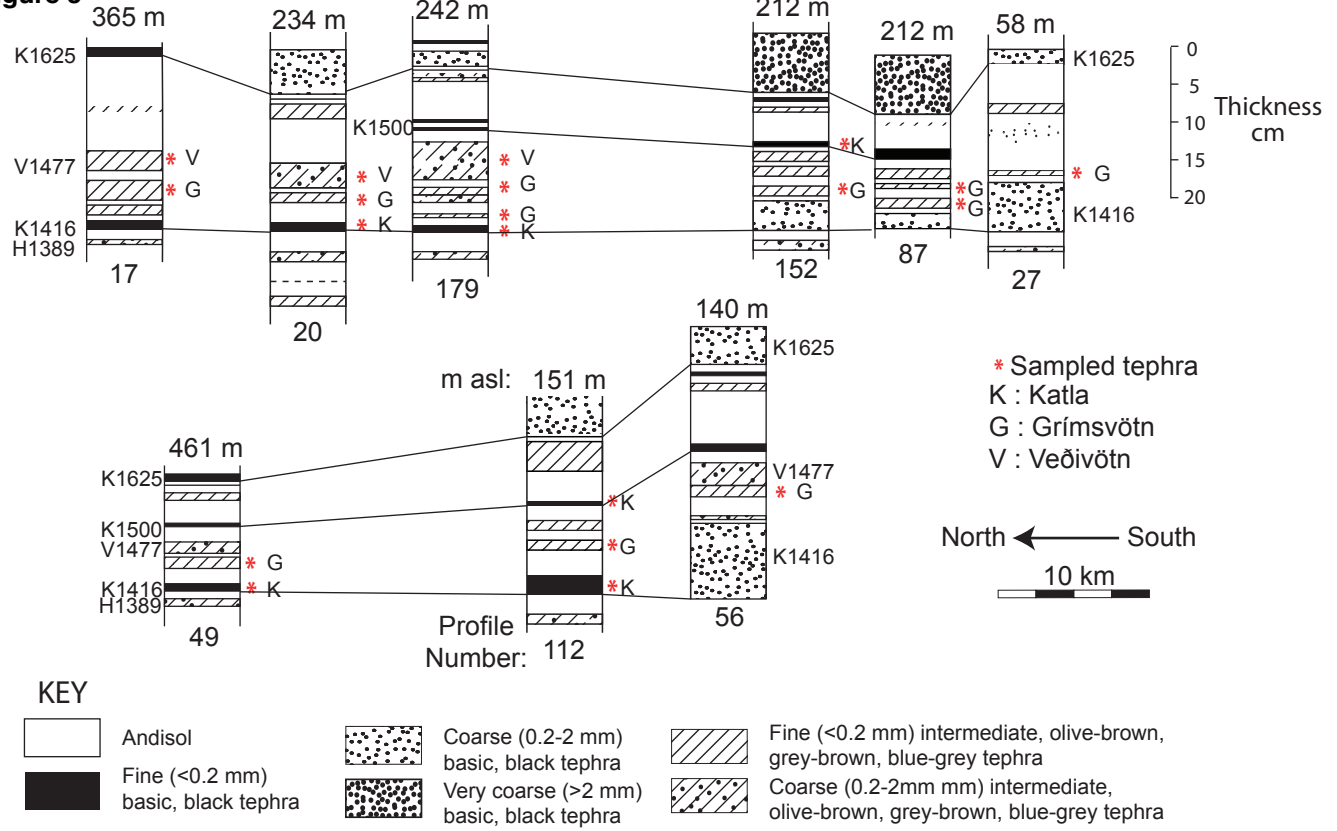
365 m
234 m
242 m
212 m
212 m
58 m
K1625
V1477
K1416
H1389
K1500
V
G
K
17
20
179
152
87
27
0
5
10
15
20
Thickness
cm
461 m
m asl:
151 m
140 m
49
112
56
Profile
Number:
* Sampled tephra
K : Katla
G : Grímsvötn
V : Veðivötn
North
South
10 km
KEY
Andisol
Fine (<0.2 mm)
basic, black tephra
Coarse (0.2-2 mm)
basic, black tephra
Very coarse (>2 mm)
basic, black tephra
Fine (<0.2 mm) intermediate, olive-brown,
grey-brown, blue-grey tephra
Coarse (0.2-2mm mm) intermediate,
olive-brown, grey-brown, blue-grey tephra

Figure 4

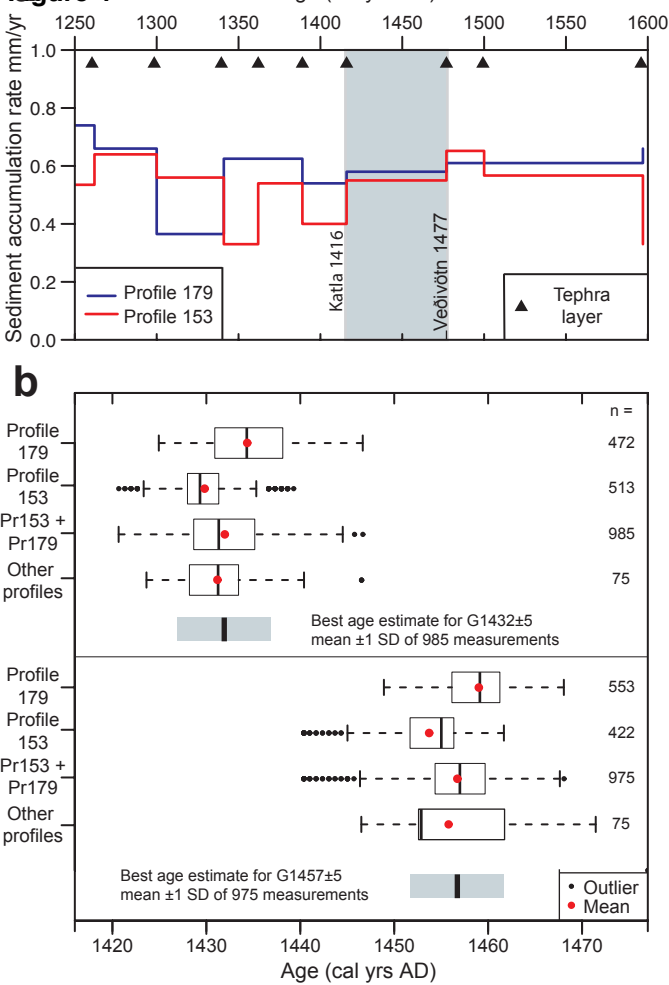
a
Age (cal yrs AD)
1250
1300
1350
1400
1450
1500
1550
1600
Sediment accumulation rate mm/yr
1.0
0.8
0.6
0.4
0.2
0.0
Profile 179
Profile 153
Katla 1416
Veðivötn 1477
Tephra layer
b
n =
Profile 179
472
Profile 153
513
Pr153 + Pr179
985
Other profiles
75
Best age estimate for G1432±5
mean ±1 SD of 985 measurements
Profile 179
553
Profile 153
422
Pr153 + Pr179
975
Other profiles
75
Best age estimate for G1457±5
mean ±1 SD of 975 measurements
Outlier
Mean
1420
1430
1440
1450
1460
1470
Age (cal yrs AD)

Figure 5

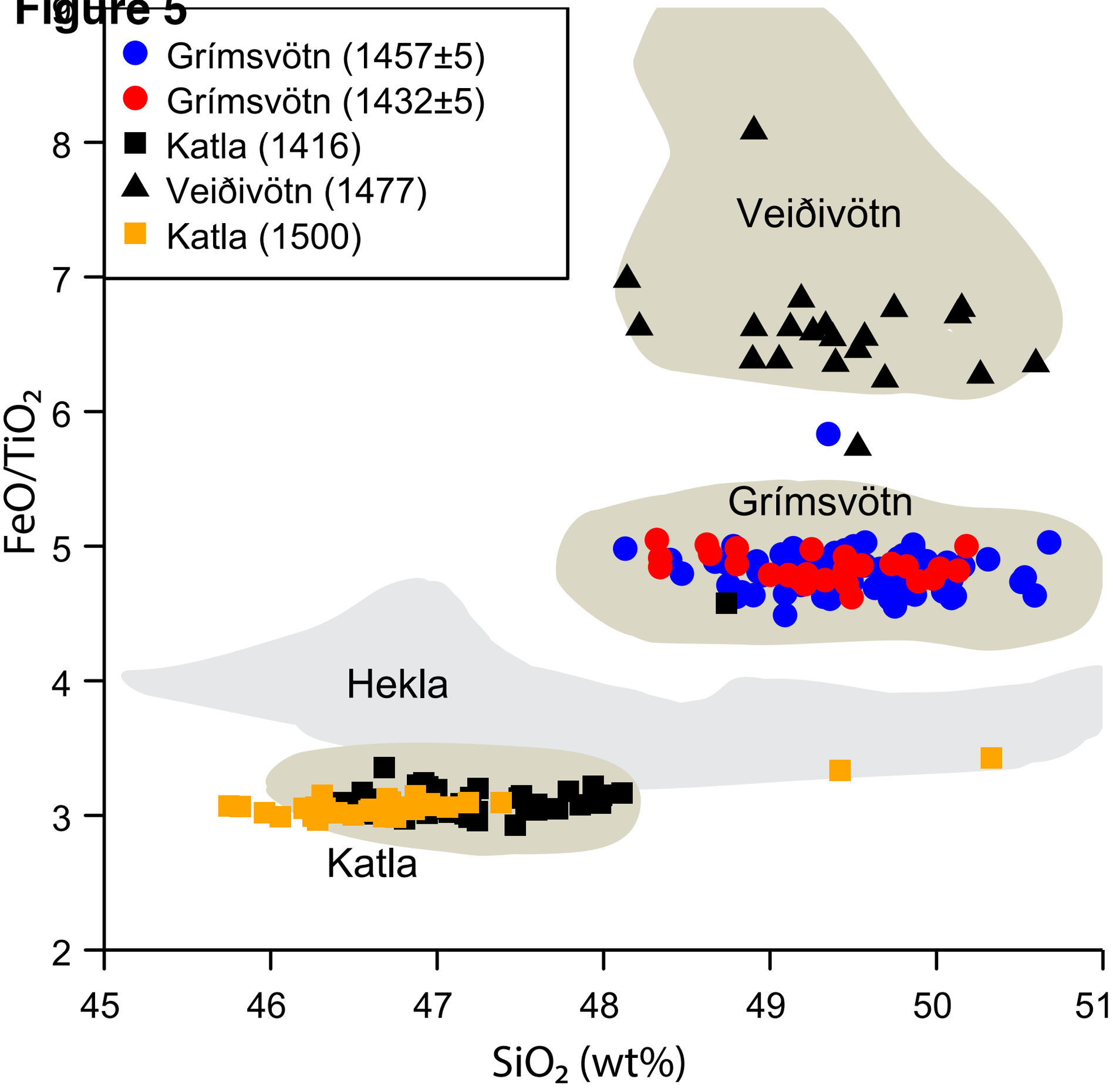
Grímsvötn (1457±5)
Grímsvötn (1432±5)
Katla (1416)
Veiðivötn (1477)
Katla (1500)
Veiðivötn
Grímsvötn
Hekla
Katla
FeO/TiO2
SiO2 (wt%)
2
3
4
5
6
7
8
45
46
47
48
49
50
51

Figure 6

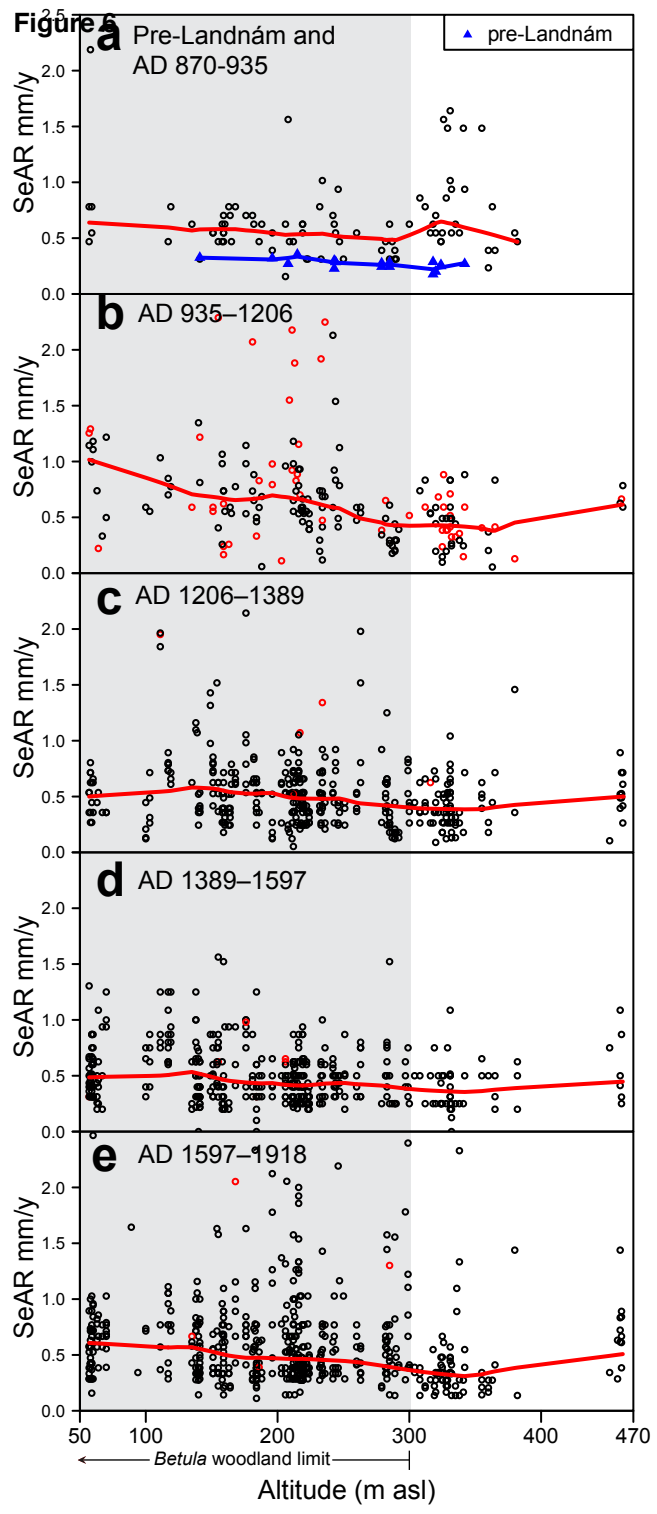
a
Pre-Landnám and
AD 870-935
pre-Landnám
b
AD 935–1206
c
AD 1206–1389
d
AD 1389–1597
e
AD 1597–1918
SeAR mm/y
0.0
0.5
1.0
1.5
2.0
2.5
50
100
200
300
400
470
Betula woodland limit
Altitude (m asl)

*Figure 7

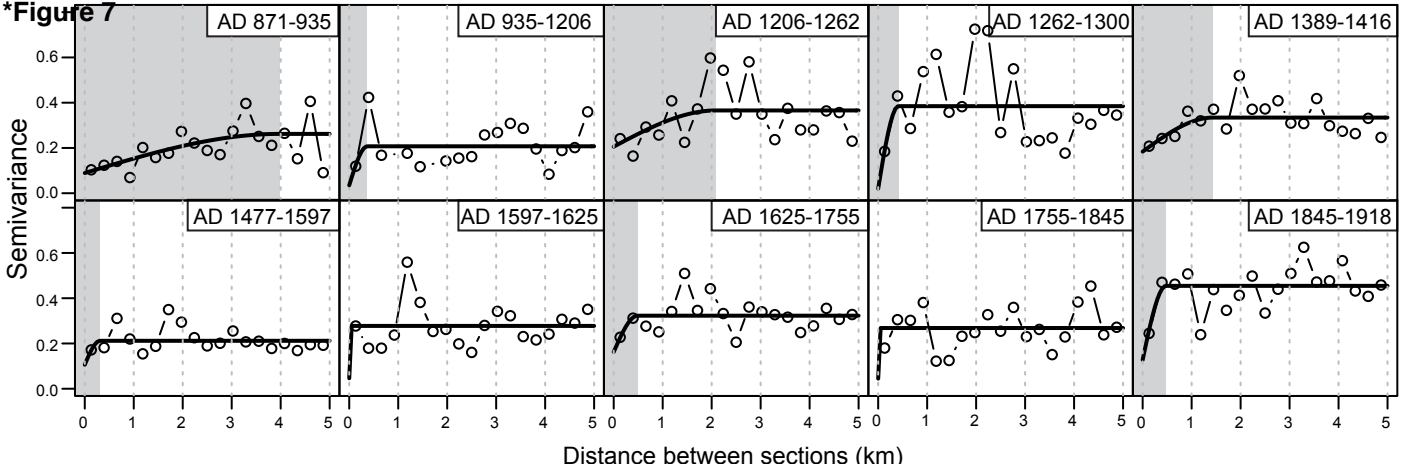
AD 871-935
AD 935-1206
AD 1206-1262
AD 1262-1300
AD 1389-1416
AD 1477-1597
AD 1597-1625
AD 1625-1755
AD 1755-1845
AD 1845-1918
Semivariance
0.0
0.2
0.4
0.6
0
1
2
3
4
5
Distance between sections (km)

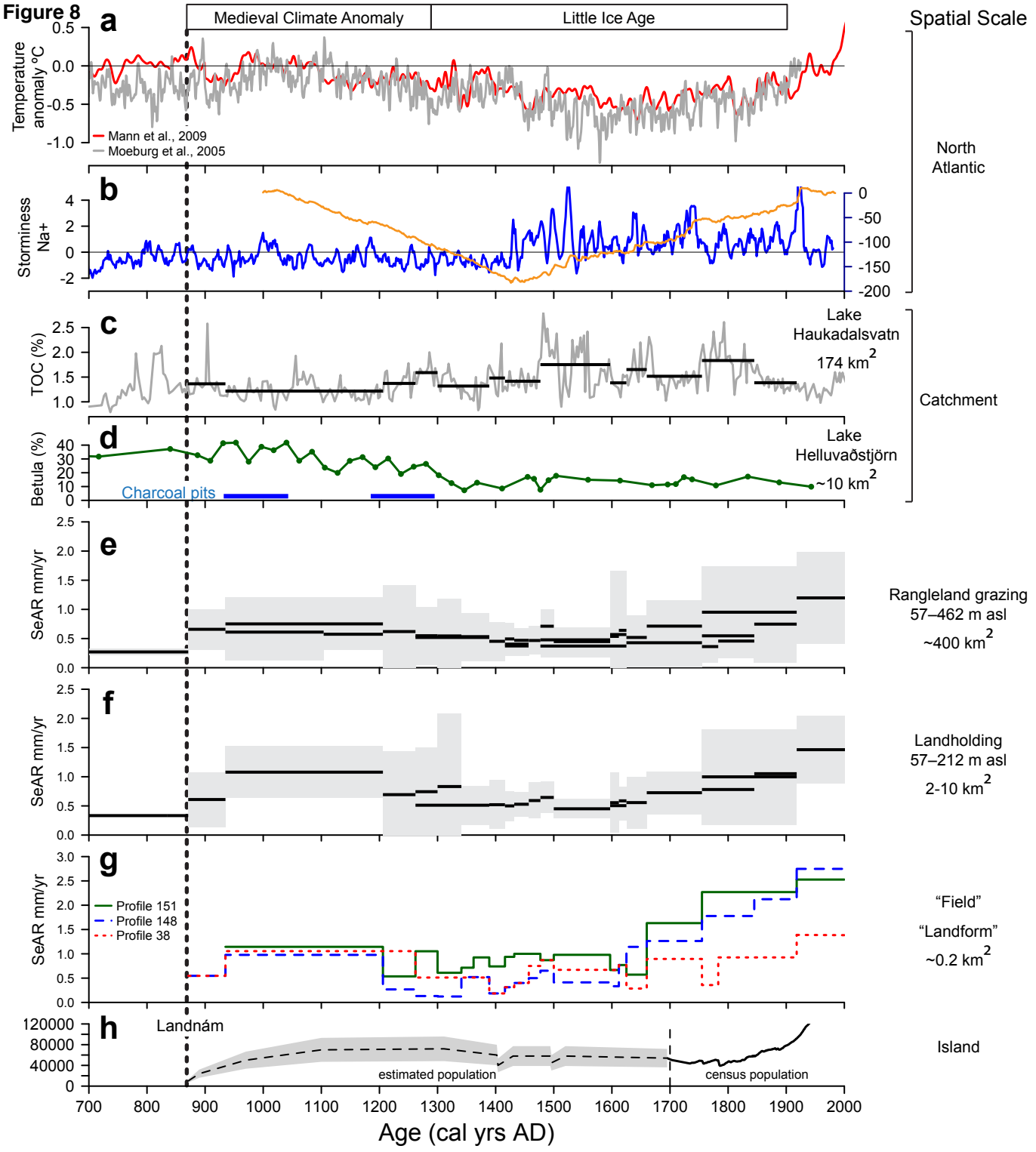
Figure 8
a
Medieval Climate Anomaly
Little Ice Age
Spatial Scale
Temperature anomaly °C
0.5
0.0
-0.5
-1.0
Mann et al., 2009
Moeburg et al., 2005
North Atlantic
b
Storminess Na+
4
2
0
-2
0
-50
-100
-150
-200
c
TOC (%)
2.5
2.0
1.5
1.0
Lake Haukadalsvatn
174 km2
Catchment
d
Betula (%)
40
30
20
10
0
Charcoal pits
Lake Helluvaðstjörn
~10 km2
e
SeAR mm/yr
2.5
2.0
1.5
1.0
0.5
0.0
Rangeland grazing
57–462 m asl
~400 km2
f
SeAR mm/yr
2.5
2.0
1.5
1.0
0.5
0.0
Landholding
57–212 m asl
2-10 km2
g
SeAR mm/yr
3.0
2.5
2.0
1.5
1.0
0.5
0.0
Profile 151
Profile 148
Profile 38
"Field"
"Landform"
~0.2 km2
h
Landnám
120000
80000
40000
0
estimated population
census population
Island
700
800
900
1000
1100
1200
1300
1400
1500
1600
1700
1800
1900
2000
Age (cal yrs AD)

Figure 9

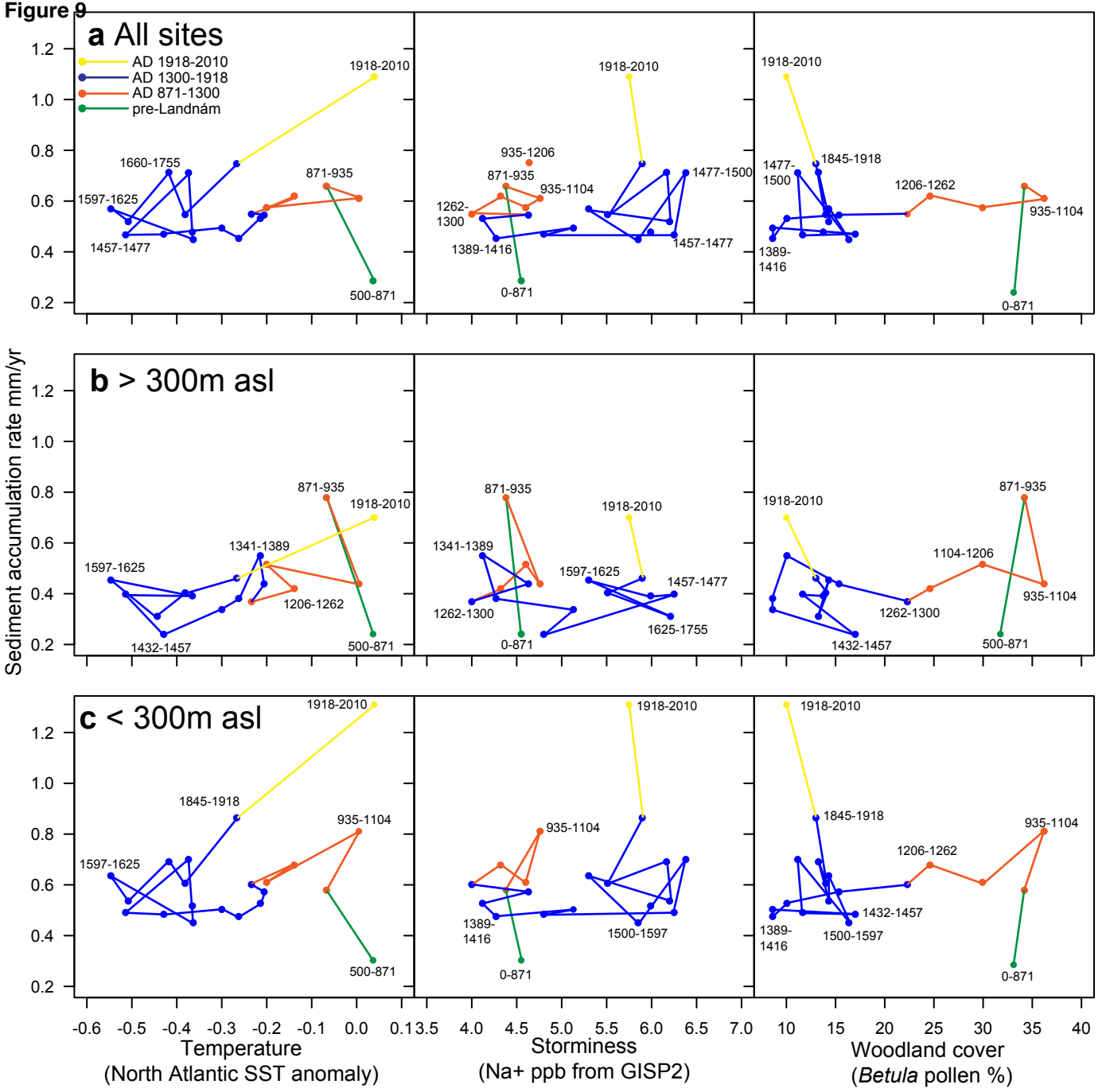
a All sites
AD 1918-2010
AD 1300-1918
AD 871-1300
pre-Landnám
1918-2010
1660-1755
871-935
1597-1625
1457-1477
500-871
935-1206
871-935
935-1104
1477-1500
1262-1300
1389-1416
1457-1477
0-871
1845-1918
1206-1262
935-1104
b > 300m asl
1341-1389
1206-1262
1432-1457
1625-1755
1104-1206
c < 300m asl
Sediment accumulation rate mm/yr
Temperature
(North Atlantic SST anomaly)
Storminess
(Na+ ppb from GISP2)
Woodland cover
(Betula pollen %)

Figure 10

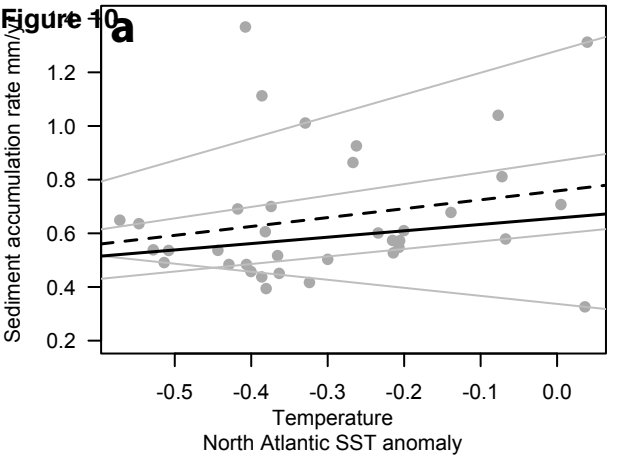
a
Sediment accumulation rate mm/yr
1.2
1.0
0.8
0.6
0.4
0.2
-0.5
-0.4
-0.3
-0.2
-0.1
0.0
Temperature
North Atlantic SST anomaly

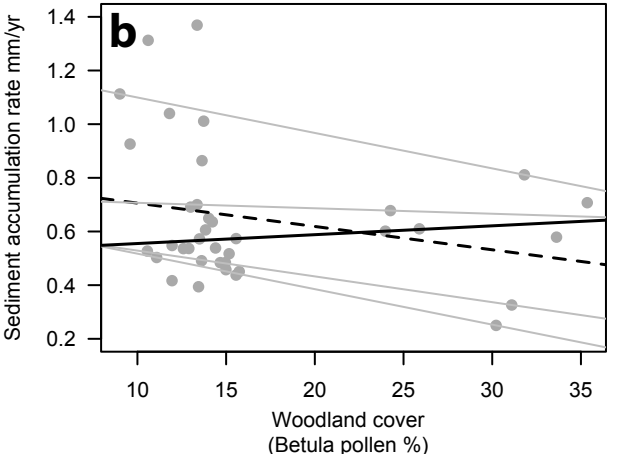
b
Sediment accumulation rate mm/yr
1.4
1.2
1.0
0.8
0.6
0.4
0.2
10
15
20
25
30
35
Woodland cover
(Betula pollen %)

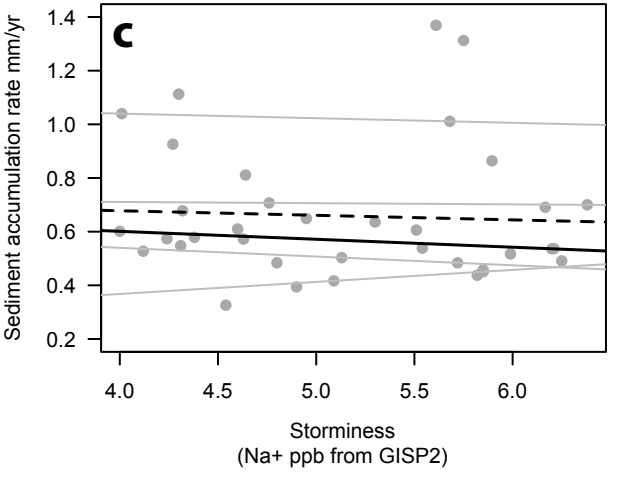
c
Sediment accumulation rate mm/yr
1.4
1.2
1.0
0.8
0.6
0.4
0.2
4.0
4.5
5.0
5.5
6.0
Storminess
(Na+ ppb from GISP2)